Laser Compression and Release Effects on Metals

Literature Review

Tané Perry Remington
Advisor: Dr. Marc A. Meyers
University of California, San Diego

Overview of Presentation

- Why people study materials at high pressures and temperatures
- Multiple methods to study metals at extreme conditions
- Overview of important laser experiments on metals
- Current and future direction of research
- Summary of main points

UCSD

Understanding the behavior of materials at high pressures and temperatures is critical for many fields of science

Planetary Interiors

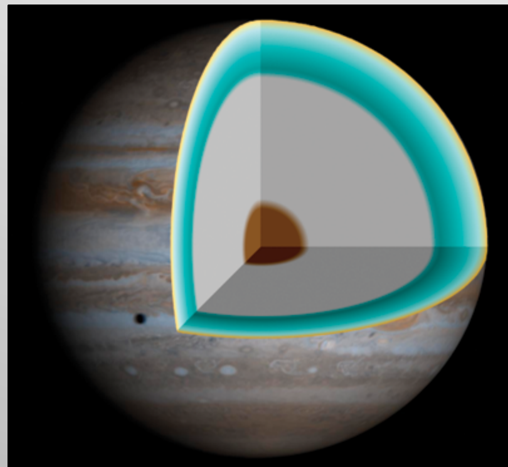

Astrophysics

Military Applications

Inertial Confinement Fusion

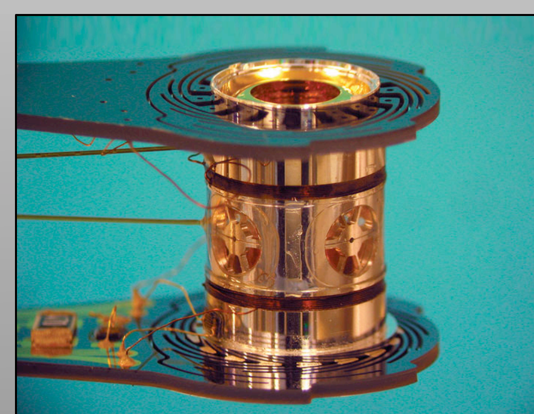

The invention of the laser 50 years ago has vastly increased our knowledge in materials behavior under compression

- Early 1950s, Nikolay Basov and Aleksandr Prokhorov independently came up with the idea of the MASER (Microwave Amplification by Stimulated Emission of Radiation)
- However it was Charles Townes, J. P. Gordon (both pictured on right), and H. J. Zeiger who built the first MASER

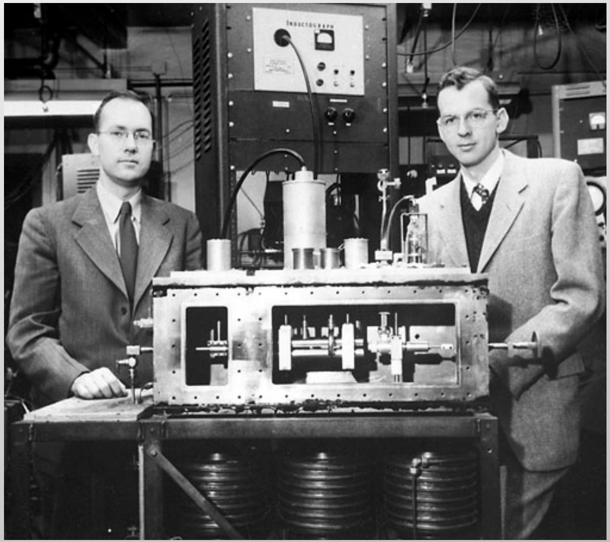

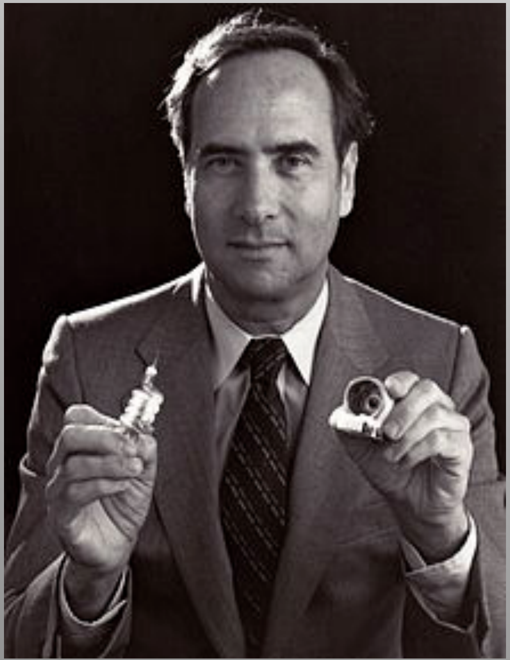

In 1960, Theodore H. Maiman at Hughes Research Laboratories operated the first functioning ruby LASER (Light Amplification by Stimulated Emission of Radiation)

-Currently the most well-known laser facilities include: LLNL Jupiter, LLNL NIF, LLE OMEGA, LANL Trident

-Over the past 50 years of materials science research, strain rates below 10^6 s^{-1} have been studied in-depth

-Now scientists are trying to characterize deformation mechanisms in the extreme regime of pressures, temperatures and strain rates above 10^6 s^{-1}

NIF has 192 laser beams with the capability of reaching 4×10^6 Joules in 5×10^{-9} seconds

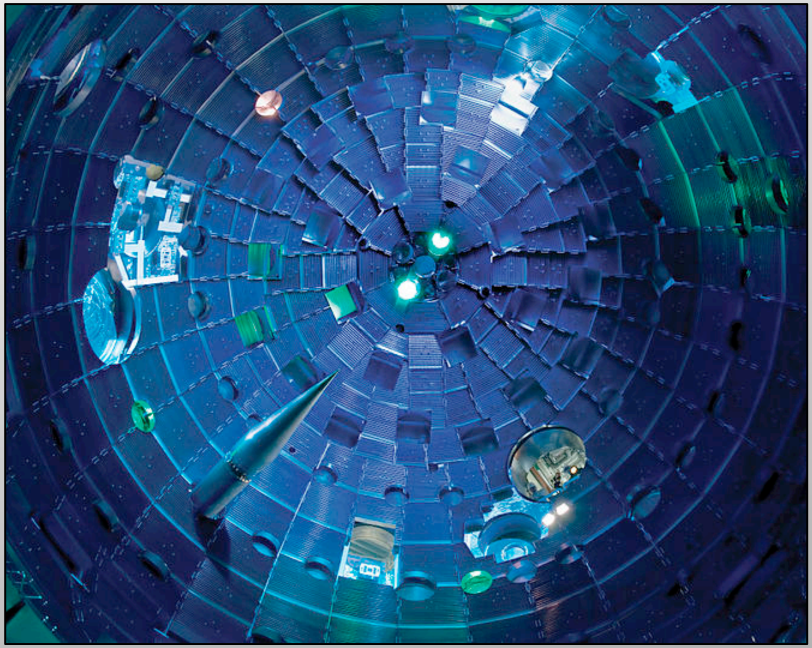

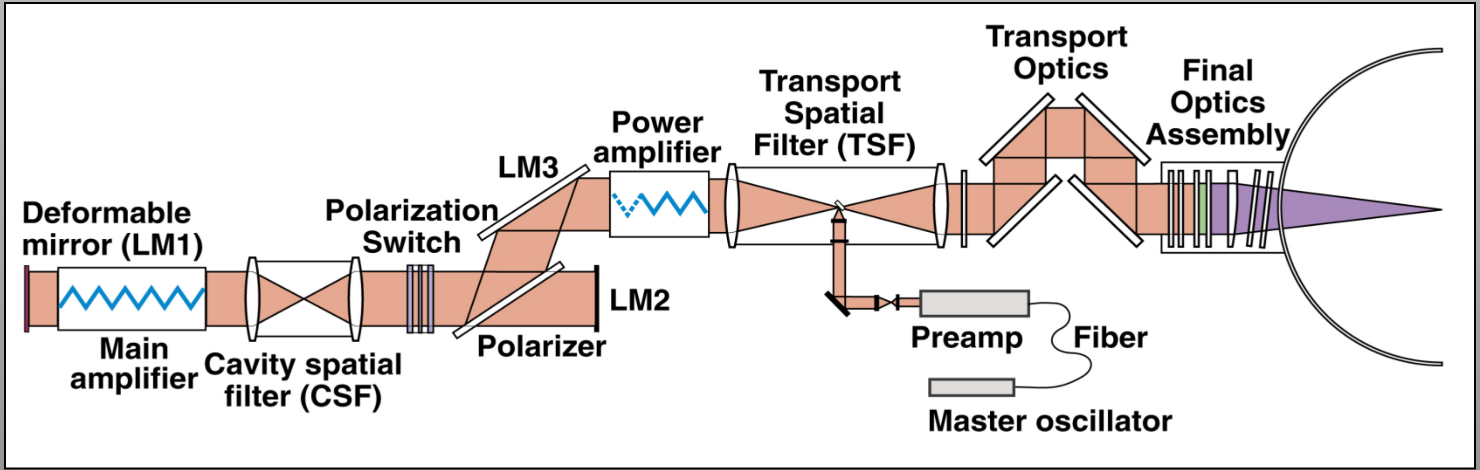

Several methods have been developed to study materials at high pressure

HE flyer plate configuration

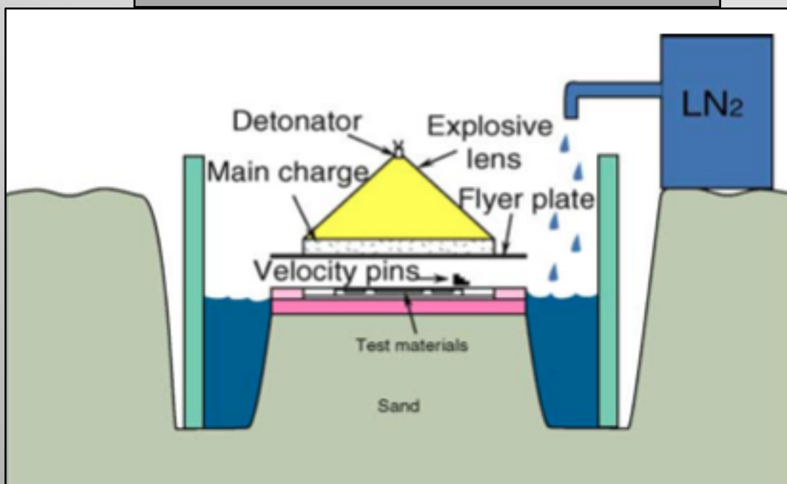

Explosive configuration for generating a HE shock in the metal

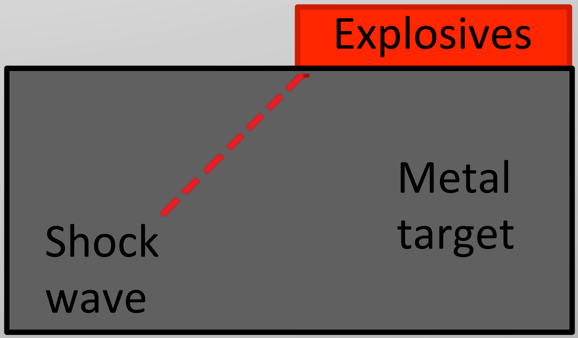

Gas gun configuration

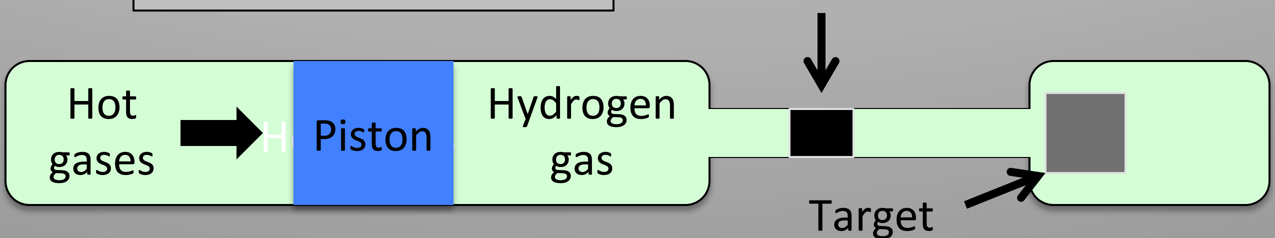

Depending on the type of research certain methods pose advantages over others

Method	Pressure Range	Time	Sample Size	Application
Large Volume Press	1 Pa	microsecond - millisecond	500 mm	Planetary interiors
Diamond Anvil Cell	300 GPa	nanosecond	20 um	Crystallographic studies
Gas Gun	10 GPa	microsecond	25-100 mm dia	HEL, spallation and strain rate
Explosive	14 GPa	microsecond	Bulk material	Physical processes
Flyer Plate	250 GPa	microsecond	400-700 um thickness	Physical processes
Laser	5000 GPa	nanosecond - picosecond	2-3 mm dia	Phase transitions, high strain rates, min annealing

Laser shock can produce a variety of defects: voids, phase transitions, dislocations and release in solids

Shock Loading

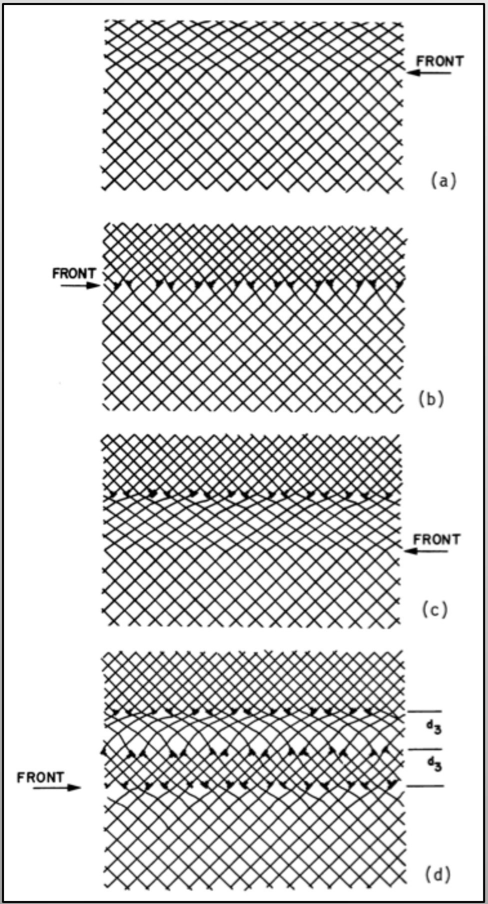

Propagation of a shock front through a crystal

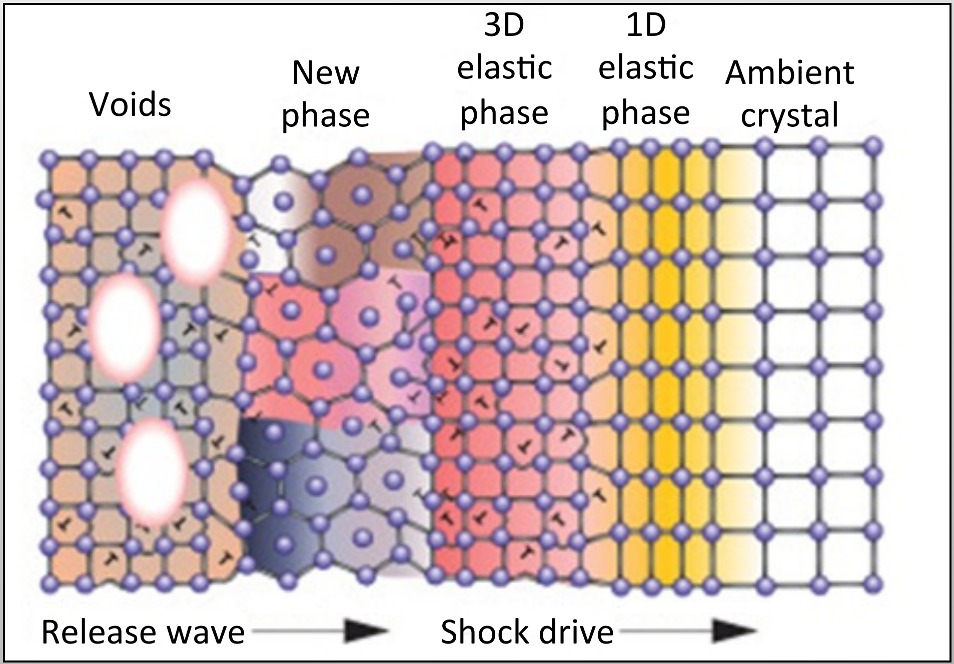

There are 2 ways to launch a shock wave:

1) Directly launch a square pulse shock wave and hold constant intensity
2) Shield sample with plastic but no reservoir

A.H. Clauer et al., Shock Waves and High-Strain-Rate Phenomena in Metals, ed. M.A. Meyers and L.E. Murr (New York: Plenum Press, 1981), p. 675-702; https://www.llnl.gov/str/JulAug06/Lorenzana.html

The Principal Hugoniot Equations give experimental results (ρ and T) from shock laser experiments

[Figure courtesy of Ray Smith and Jean-Paul Davis]

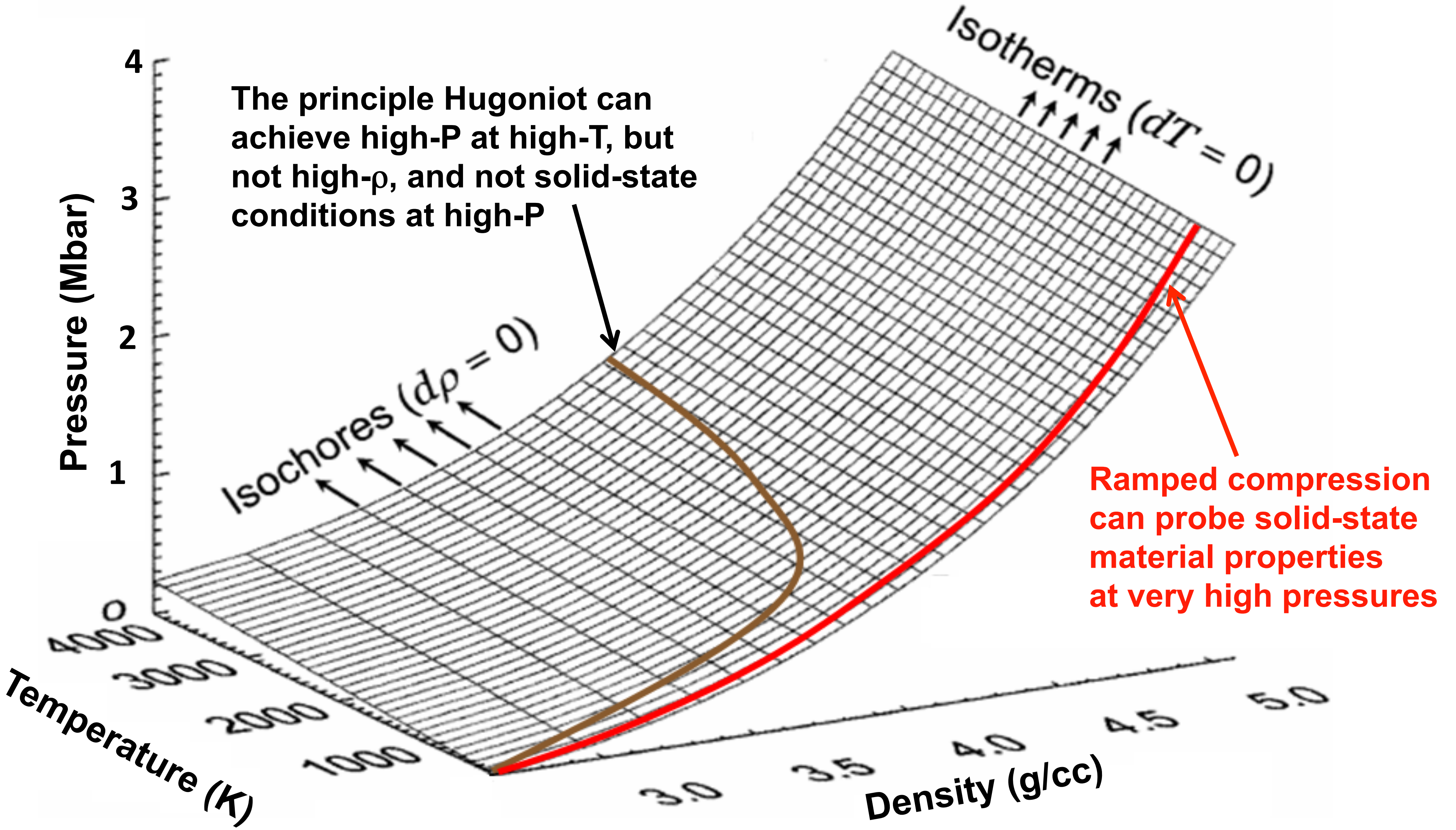

Ramp loading is another form of laser compression also known as “quasi-isentropic”

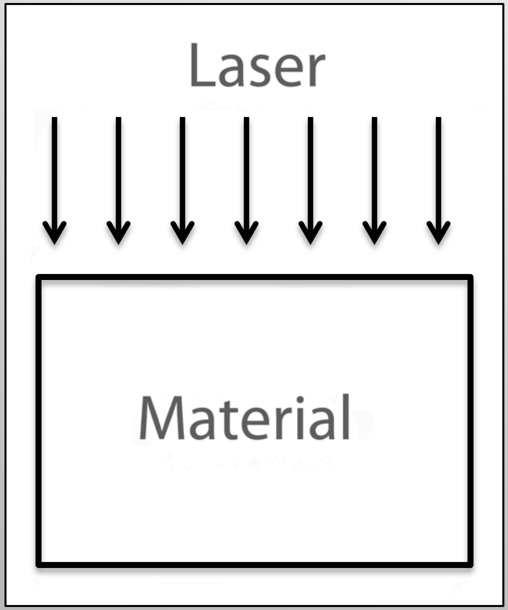

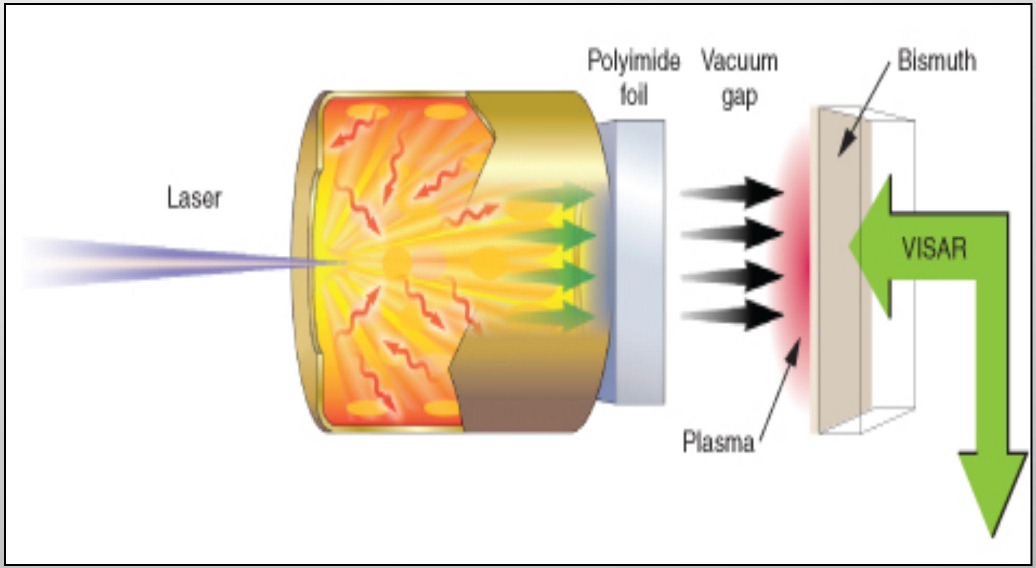

Target design for laser-driven ramp compression of bismuth foil

There are 2 ways to launch a ramp wave:

1) Directly drive the sample and create pressure vs. time by shaping laser pulse
2) Use laser to launch shock through sacrificial plastic with gap, the amplitude of the pressure will decay as it travels through the material

Can only maintain 100um of ramp wave into sample

In 1963 shock pulses were generated in metals from laser-pulse induced vaporization at the surface

- Askaryon and Morez's technique was advanced
- Shortly after, White et al were able to show temperature distributions for different types of laser pulses and energy
- Allowed Hugoniot data for a broad range of pressures to be obtained

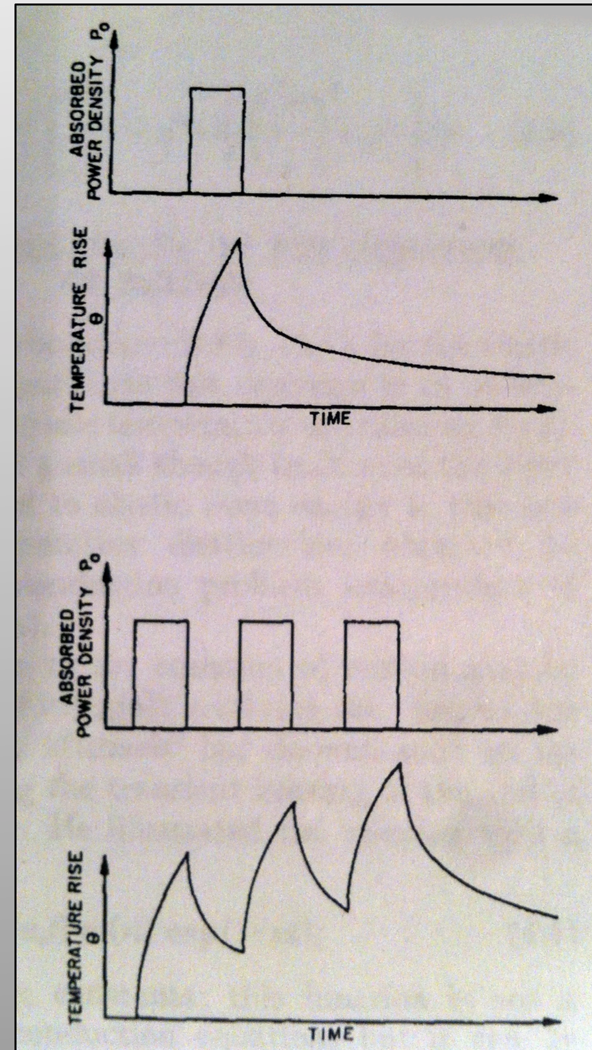

G.A. Askaryon and E.M. Morez, *JETP Lett.,* 16 (1963), p. 1638
R.M. White, J. Appl. Phys. 34, 2123 (1963)

A pulsed, high power laser beam was used to create "blow-off" plasmas at surface of solid materials

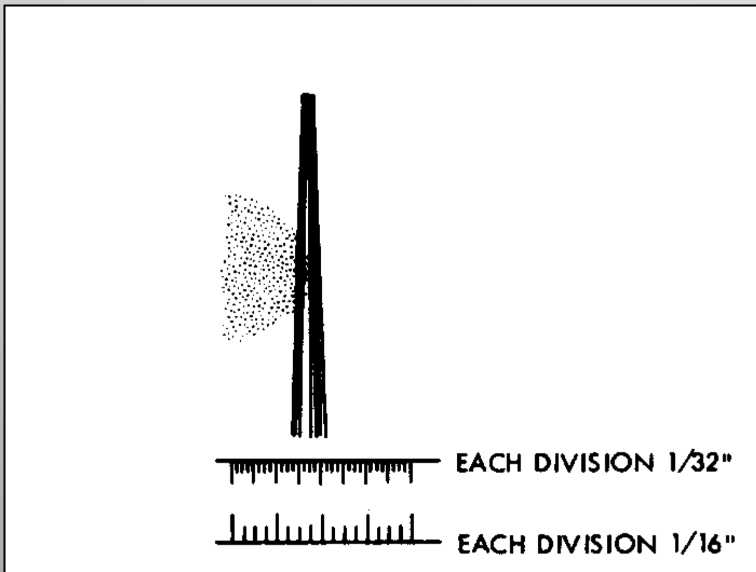

Figure: A polaroid image of a laser pulse hitting a target

- The laser used was an oscillator-amplifier configuration of neodymium doped glass rods capable of emitting pulses having powers up to a gigawatt (60 J in 60 ns), pressure 10^{-6} torr
- By conservation of momentum, a stress pulse is induced in the target causing it to deform at the free surface at a time depending upon the shock wave velocity
- Produces stress pulses in tenths of Mbar
- Discovered vacuum was necessary to unshield targets from incident laser light

C.H. Skeen and C.M. York, *Laser-Induced "Blow-Off" Phenomena*, Applied Physics Letters, 1968

In 1970, Anderholm introduced laser-transparent overlays

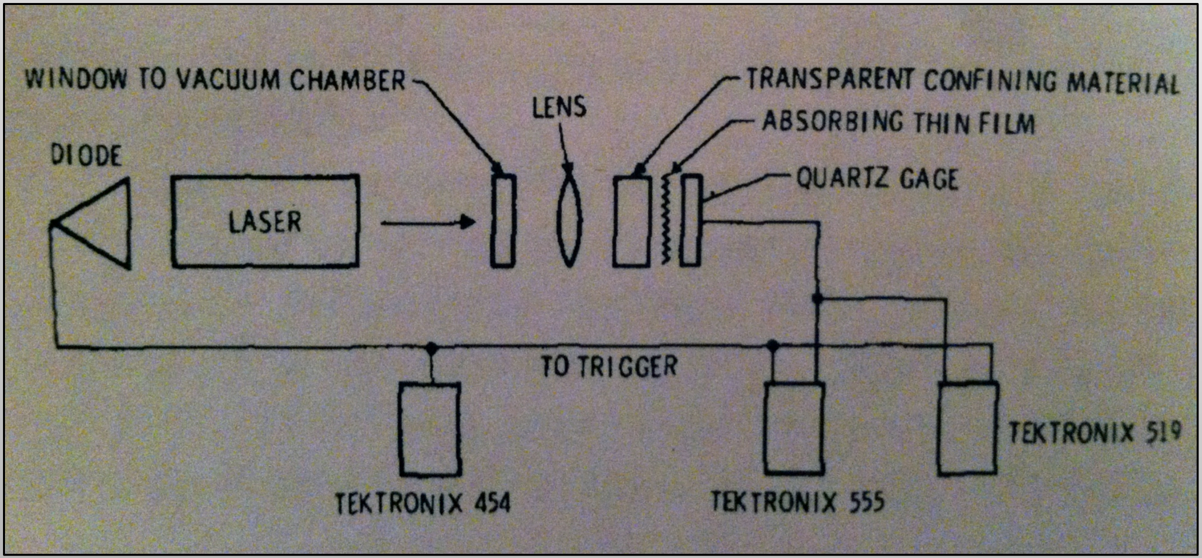

Schematic of the experimental configuration

- This enabled the confinement of the vapor products resulting in an increase of the peak pressure of the shock incident on the metal
- Created stress waves with a peak pressure of 34 kbar using the blow off concept paired with the thin film absorber

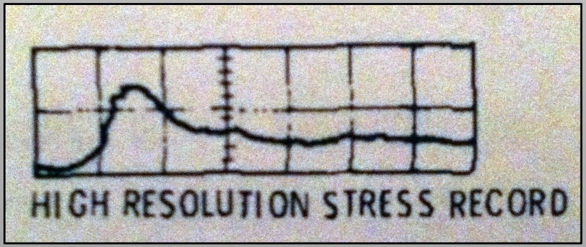

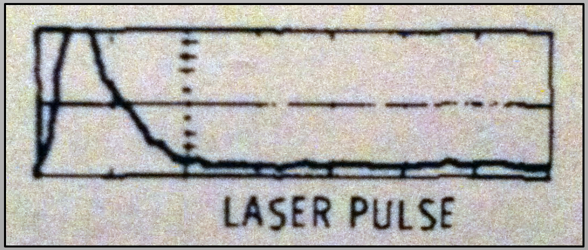

Duration of the applied stress is comparable to laser duration

N.C. Andelholm, *Appl. Phys. Lett.*, 16 (1970), p. 113

In 1978 Inal and Murr used Q-switched laser beams to study lattice defects in molybdenum and tungsten wires

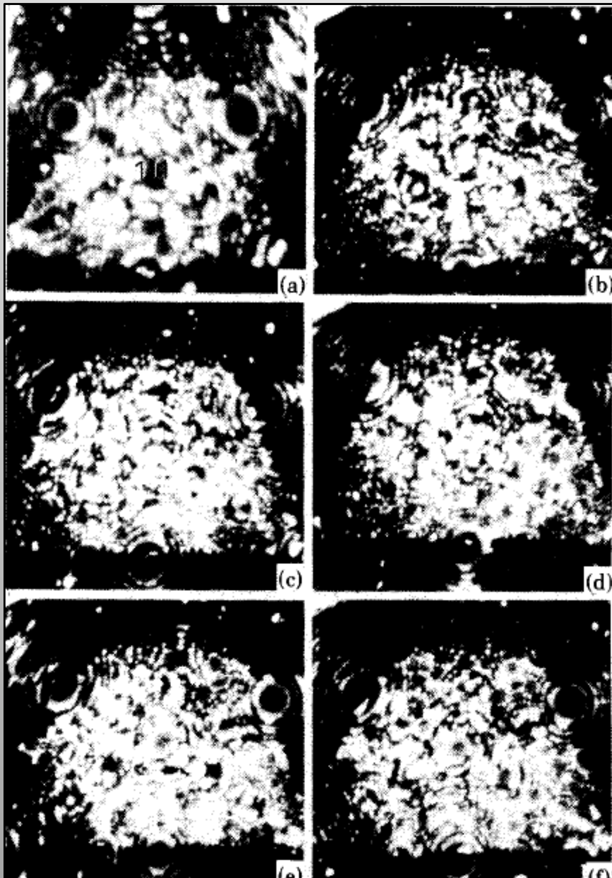

Vacancy concentration increases with increasing energy

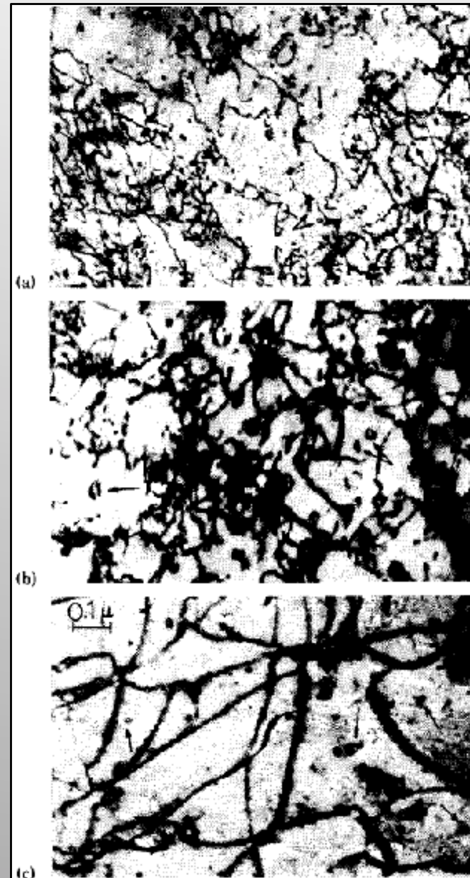

Dislocation density increases with increasing pressure

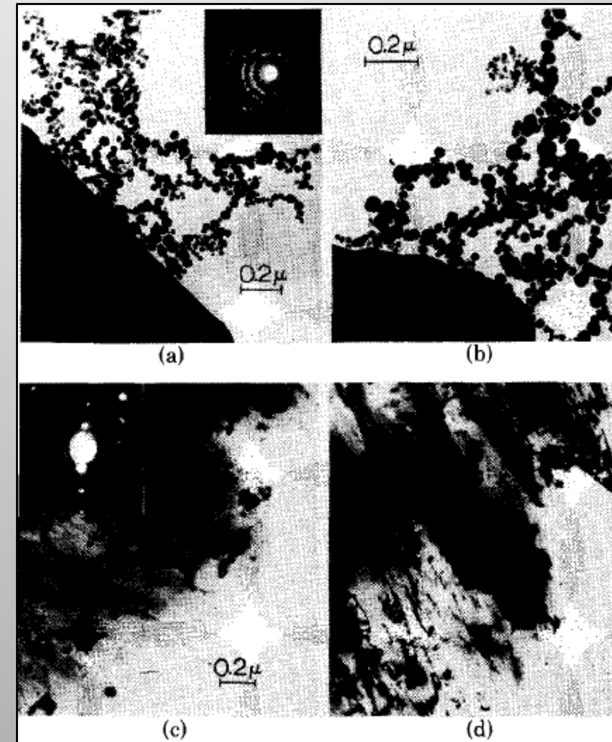

Oxidation bead strings at melting

O.T. Inal and L.E. Murr, *Laser-shock-induced microstructural changes and a comparison with explosive-shock-induced phenomena in metals: Field-ion and electron microscopic studies*, J. Appl. Phys., 1978

Inal and Murr also demonstrated the difference between laser and explosive shock propagation

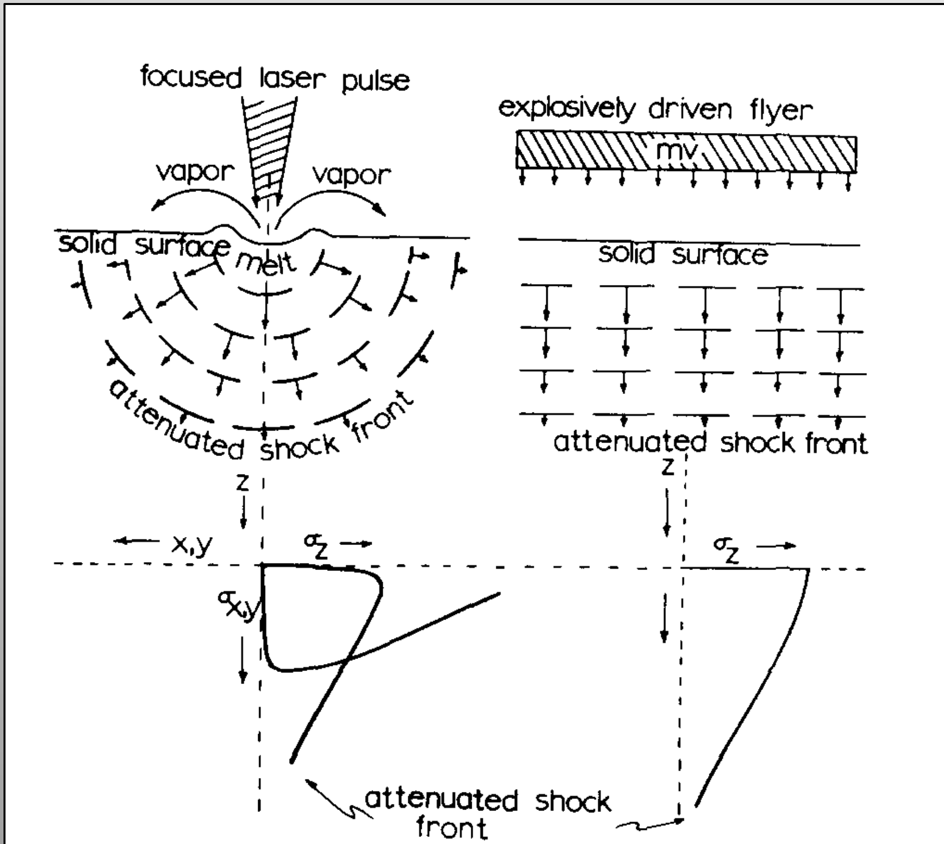

- Schematic comparison of laser-generated and explosively generated shock waves in a solid. The laser beam direction and the flyer-plate direction are both along the *z* axis.
- Laser shocks will propagate from a small source region creating a radially attenuated stress pulse
- Conventional shock loading creates planar (uniaxial-strain) shocks through the sample
  - In most cases the uniaxial-strain is not large and allows for hydrostatic stress approximations

*This schematic is for shock propagation through a thick sample

O.T. Inal and L.E. Murr, *Laser-shock-induced microstructural changes and a comparison with explosive-shock-induced phenomena in metals: Field-ion and electron microscopic studies*, J. Appl. Phys., 1978

In 1980 Clauer et al. used laser-induced shock pulses to modify crystal structures to increase their hardness and fatigue life

Surface harndess profiles across the laser shocked zone on aluminum. Peak shock pressure at 5.8 GPa with a 25 usec laser pulse

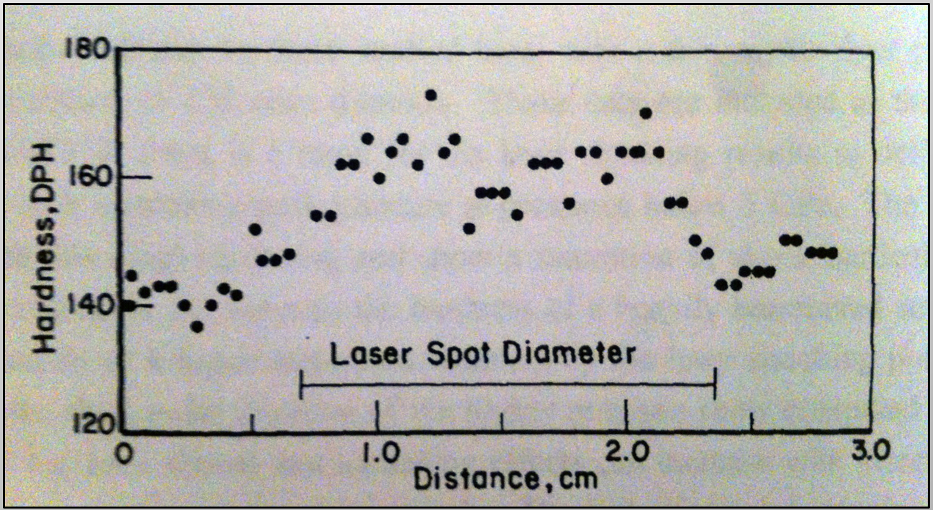

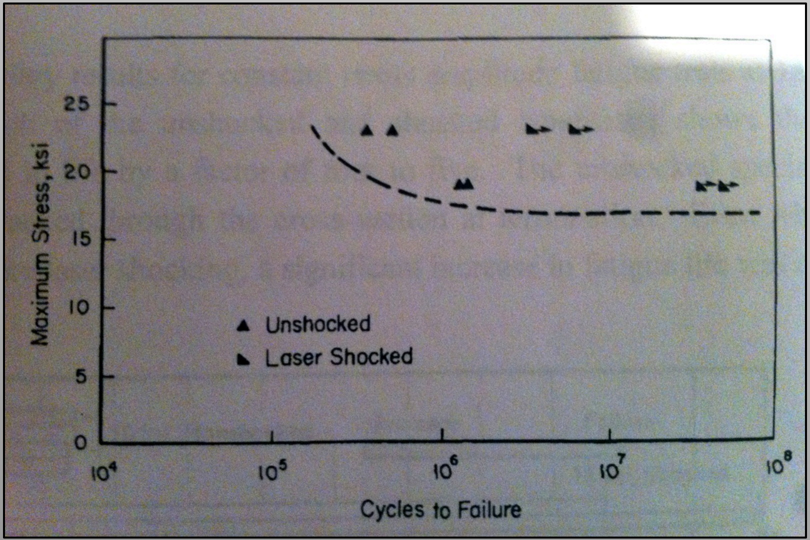

Effects of laser shocking on the fatigue life of welded aluminum for axial fatigue tests. Dashed line represents typical as-welded property.

A.H. Clauer et al., Shock Waves and High-Strain-Rate Phenomena in Metals, ed. M.A. Meyers and L.E. Murr (New York: Plenum Press, 1981), p. 675-702.

In 1980 Clauer et al. used laser-induced shock pulses to modify crystal structures to increase their hardness and fatigue life

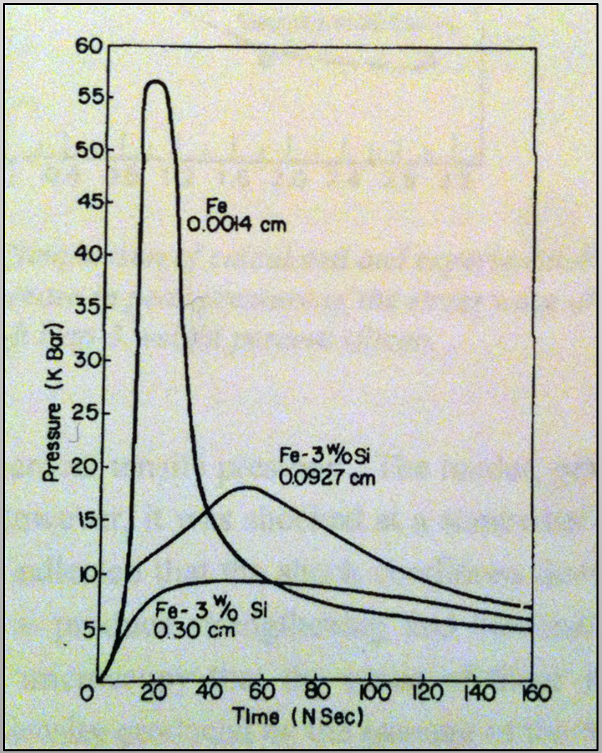

Stress wave profiles after passing through iron ad iron alloy of increasing thickness

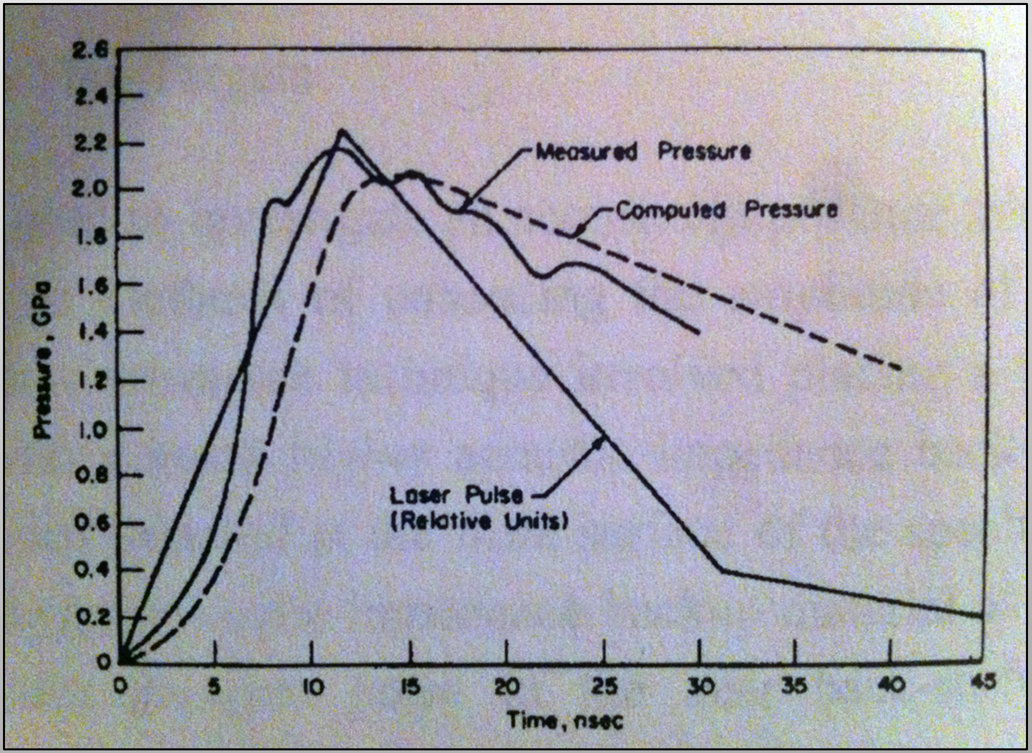

Comparison of computed and measured pressures for water overlay aluminum target at 1.2 x 10^9 W/cm^2

A.H. Clauer et al., Shock Waves and High-Strain-Rate Phenomena in Metals, ed. M.A. Meyers and L.E. Murr (New York: Plenum Press, 1981), p. 675-702.

Laser shock compression on monocrystalline copper created dislocation tangles, twins and stacking faults

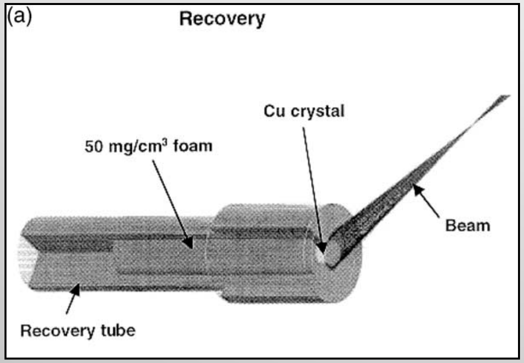

Left: Recovery tube for Cu crystal

Right: Laser drive setup

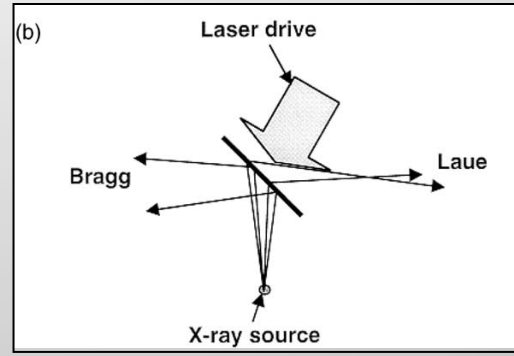

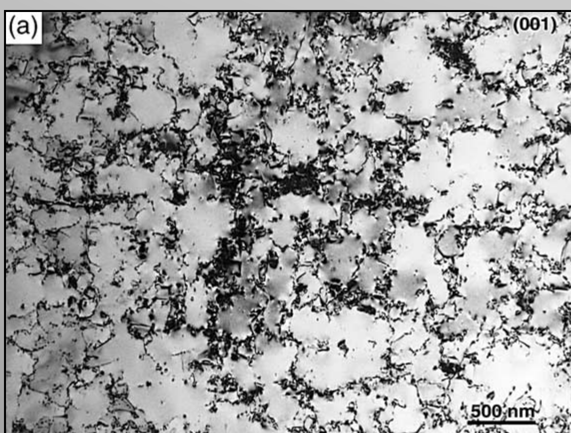

Dislocation substructure for Cu (100) shocked at 40 J

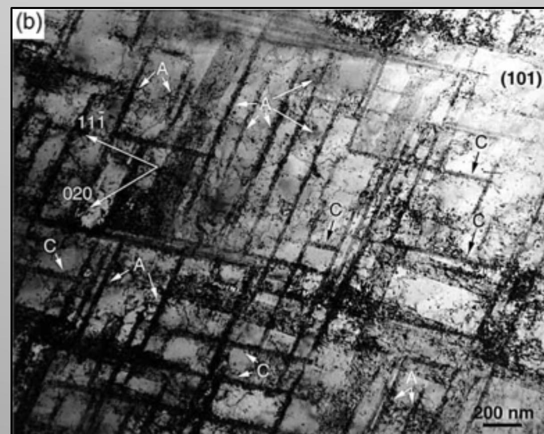

Stacking fault for Cu (100) shocked at 205 J

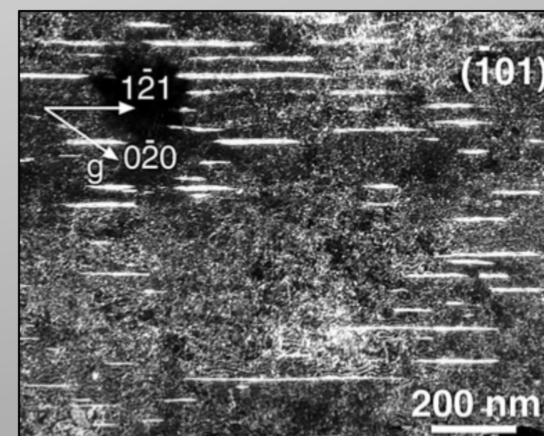

Mico-twins for Cu (100) shocked at 320 J

M.A. Meyers a,*, F. Gregori b, B.K. Kad a, M.S. Schneider a, D.H. Kalantar c, B.A. Remington c, G. Ravichandran d, T. Boehly e, J.S. Wark f, Laser-induced shock compression of monocrystalline copper: characterization and analysis, Acta Materialia 51 (2003) 1211–1228

Laser shock compression on monocrystalline copper created dislocation tangles, twins and stacking faults

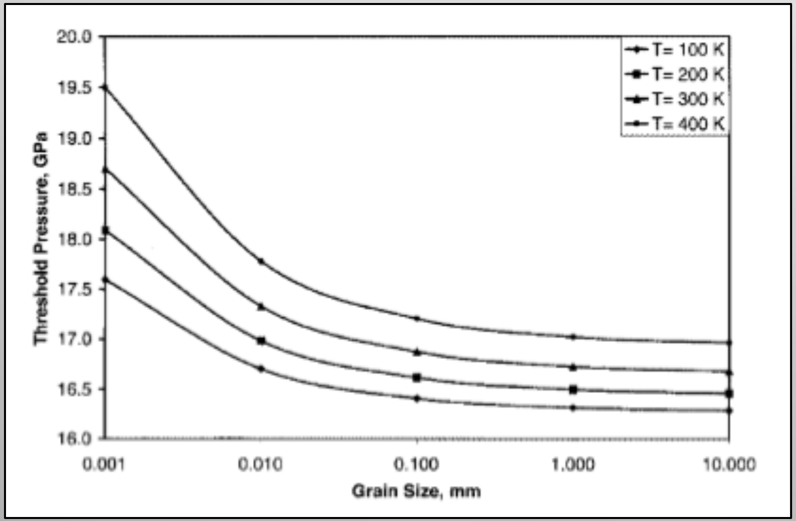

Predicted threshold stress for the initiation of twinning as a function of initial temperature and grain size

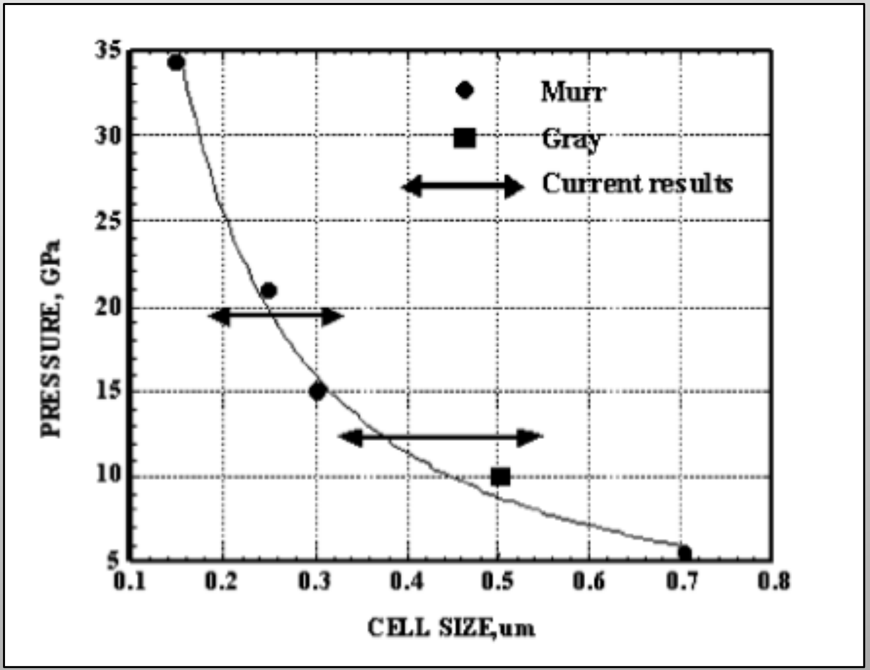

Cell size as a function of pressure for shock loaded Cu

M.A. Meyers a,∗, F. Gregori b, B.K. Kad a, M.S. Schneider a, D.H. Kalantar c, B.A. Remington c, G. Ravichandran d, T. Boehly e, J.S. Wark f, Laser-induced shock compression of monocrystalline copper: characterization and analysis, Acta Materialia 51 (2003) 1211–1228

Low, intermediate and high laser pressures on (001) and ($\bar{1}$34) single crystal copper showed orientation dependent deformation mechanisms

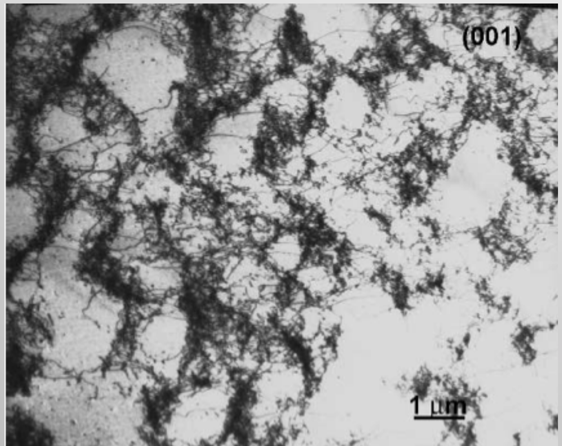

Cu (001) shocked at 20 GPa

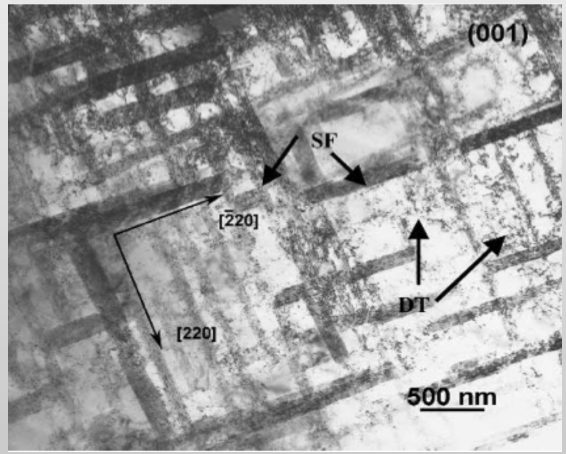

Cu (001) shocked at 40 GPa

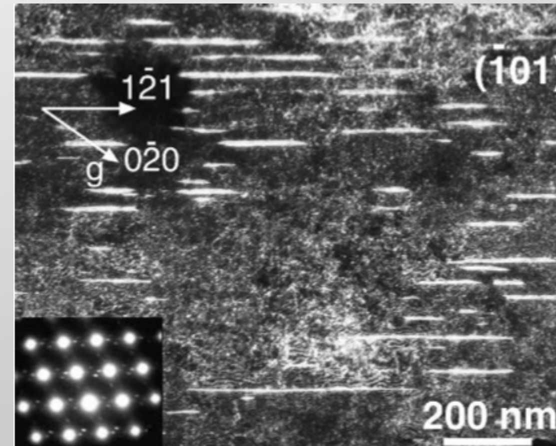

Cu (001) shocked at 60 GPa

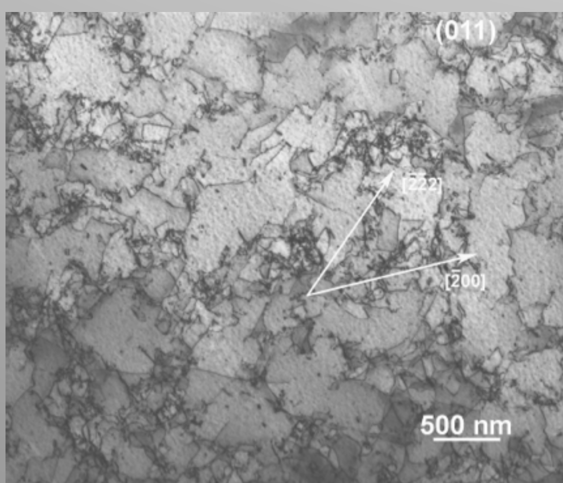

Cu ($\bar{1}$34) shocked at 20 GPa

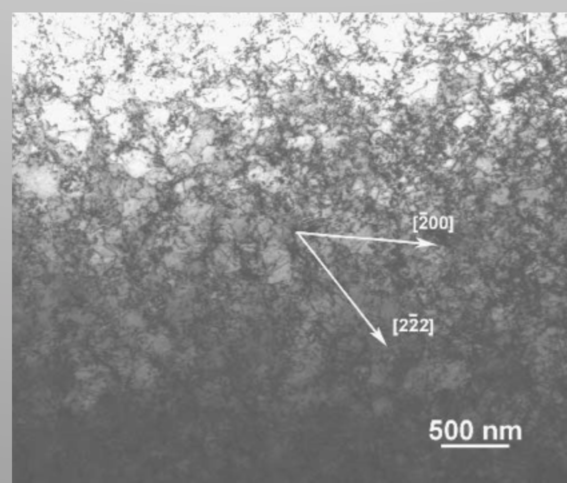

Cu ($\bar{1}$34) shocked at 40 GPa

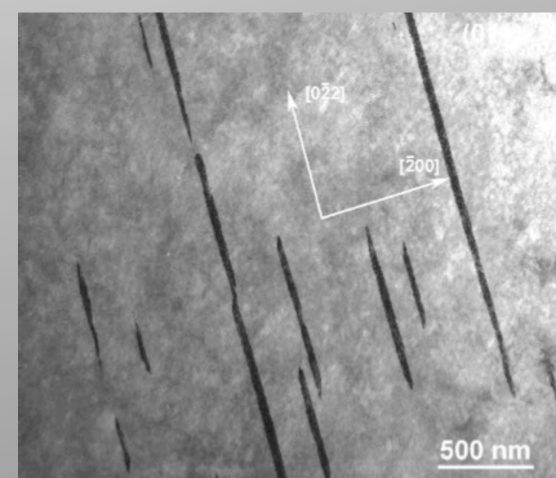

Cu ($\bar{1}$34) shocked at 60 GPa

M.S. Schneider, B.K. Kad, F. Gregori, B.A. Remington, M.A. Meyers, Metallurgical and Materials Transactions A, 35A, 2633 (2004)

Laser shock of (001) and ($\bar{1}$34) single crystal copper showed orientation dependent slip-twinning transitions

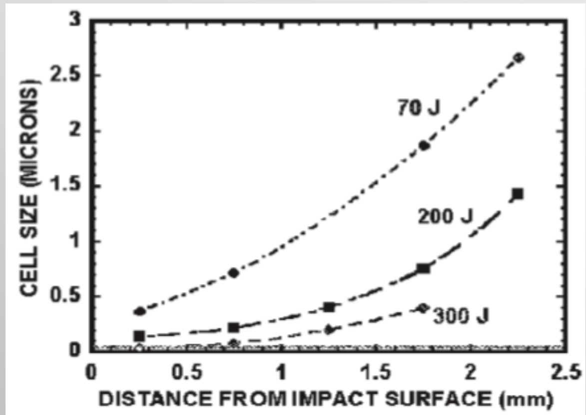

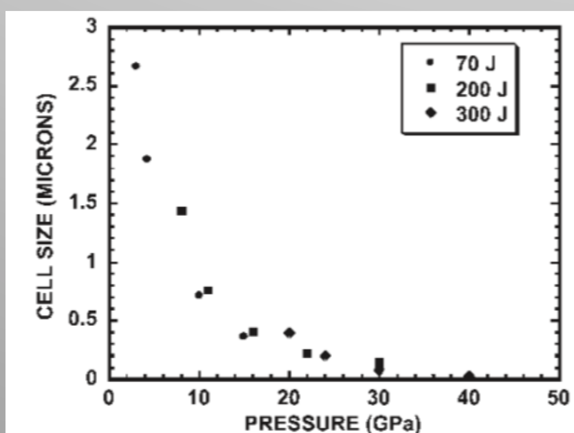

Top: Cu ($\bar{1}$34) cell size as a function of distance from impact surface. Bottom: cell size as a function of estimated pressure

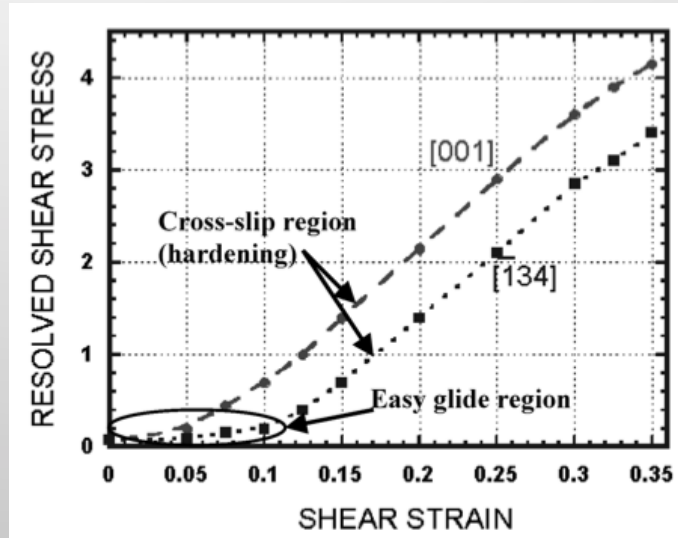

Work hardening curves obtained from Deihl for (001) and ($\bar{1}$34) Cu orientations

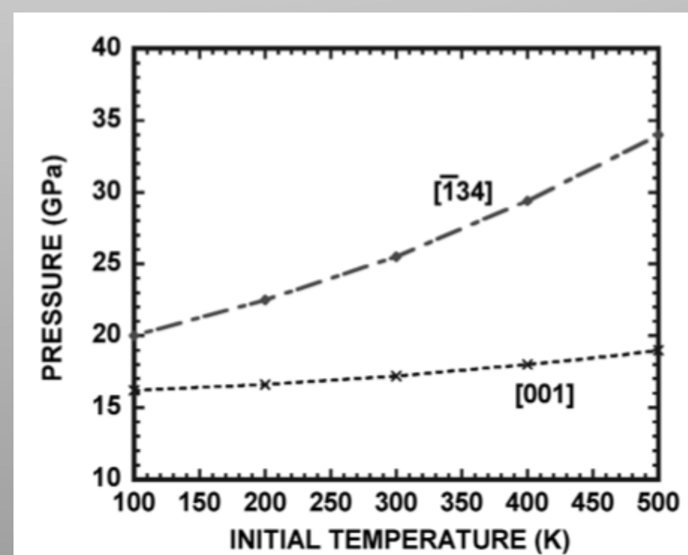

Effect of temperature on the twinning threshold pressure for (001) and ($\bar{1}$34) Cu

M.S. Schneider, B.K. Kad, F. Gregori, B.A. Remington, M.A. Meyers, Metallurgical and Materials Transactions A, 35A, 2633 (2004)

In 2005 Cao et al showed that microstructure defect in single crystal copper was dependent on shock compression method

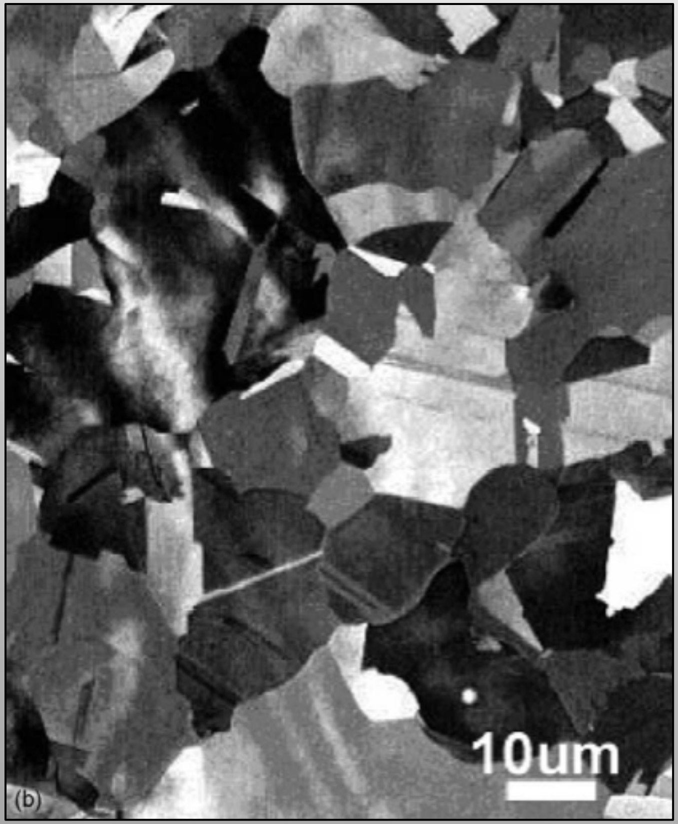

Recrystallized grains observed in HE plate-impacted Cu (001) and (221) at 57 GPa but not observed in laser shocked samples

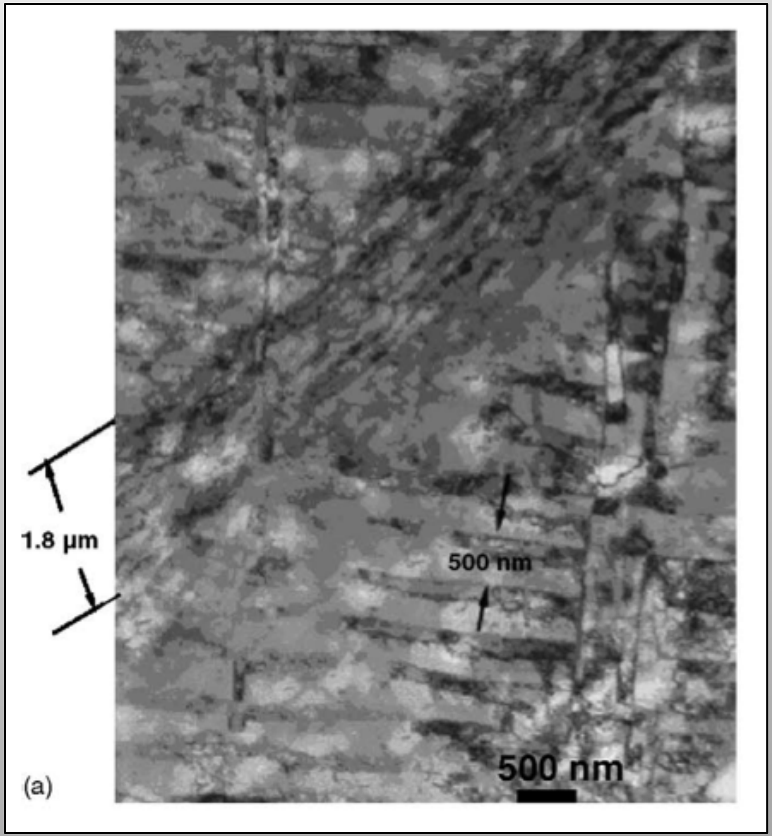

Localized shear bands were observed in HE plate-impact shock but are absent in samples laser shocked

B.Y. Cao, D.H. Lassila, M.S. Schneider, B.K. Kad, C.X. Huang, Y.B. Xu, D.H. Kalantar, B.A. Remington, M.A. Meyers, Mats Sci A, 409 (2205)270

In 2008 Jarmakani et al used MD to simulate slip-twinning transition pressures in nano and mono crystalline Ni and compared to experimental and analytical calculations

Monocrystalline Ni

- MD showed partial dislocation loops emitted at shock front along {111} slip systems, consistent with Meyers homogeneous dislocation generation model
- Analytical calculations of cell-stacking fault and slip-twinning transitions are:

  cell → stacking-faults: P~27 GPa

  slip → twinning: P~15 GPa
- The defect regime as pressure is increased is:

  cells → twins

Monocrystalline Cu

- Analytical calculations cell-stacking fault and slip-twinning transitions are:

  cell → stacking-faults: P~5 GPa

  slip → twinning: P~50 Gpa
- The defect regime as pressure is increased is:

  cells →staking faults → twins

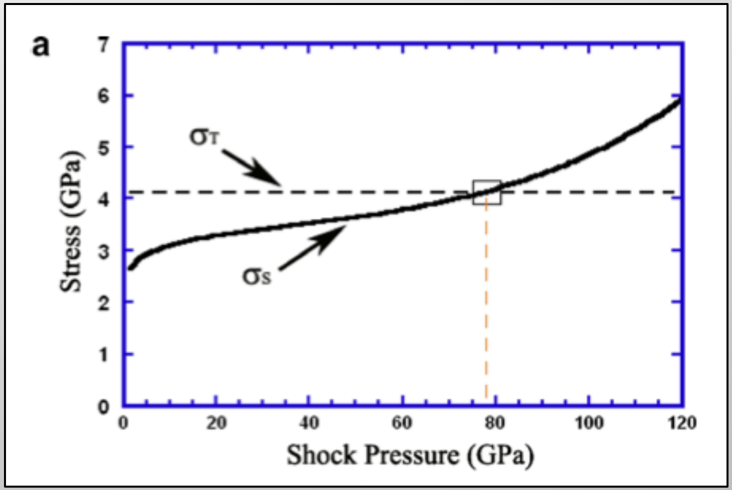

- The above graph shows slip and twinning stress vs. shock pressure for nanocrystalling Ni

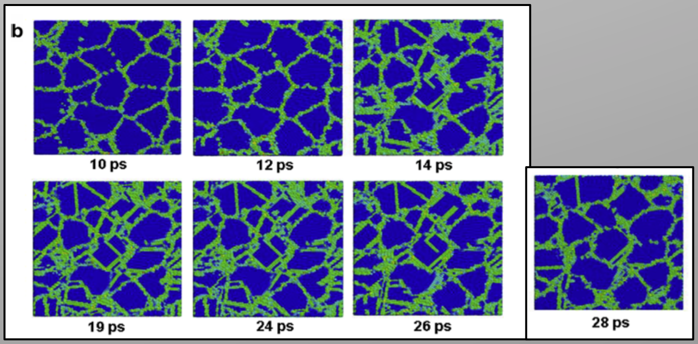

H.N. Jarmakani, E.M. Bringa, P. Earhart, B.A. Remington, V. Nhon and M.A. Meyers, Molecular Dynamics Simulations Of Shock Compression Of Nickel: From Mono to Nano-Crystals, Acta Mat, 2008, 56, 5584-5604.

In 2003 Preston, Tonks and Wallace present a model of metallic plastic flow for numerical simulations of explosive loading and high velocity impacts

Arrhenius Equation showing dislocation transition rate:

$$\dot{\psi} = \dot{\psi}_0 \exp[-\Delta\Phi(\tau)/k_B T],$$

Arrhenius Equation with the addition of the inverse error function:

$$\hat{\tau}_s = s_0 - (s_0 - s_\infty)\mathrm{erf}[\kappa \hat{T} \ln(\gamma \dot{\xi}/\dot{\psi})],$$

$$\hat{\tau}_y = y_0 - (y_0 - y_\infty)\mathrm{erf}[\kappa \hat{T} \ln(\gamma \dot{\xi}/\dot{\psi})].$$

These 2 equations constitute the PTW model

Voce work hardening behavior equation:

$$\frac{d\hat{\tau}}{d\varepsilon} = \theta \frac{\hat{\tau}_s - \hat{\tau}}{\hat{\tau}_s - \hat{\tau}_y}$$

Extension of Voce's equation to include experimental observations:

$$\frac{d\hat{\tau}}{d\varepsilon} = \theta \frac{\exp\left[p \frac{\hat{\tau}_s - \hat{\tau}}{s_0 - \hat{\tau}_y}\right] - 1}{\exp\left[p \frac{\hat{\tau}_s - \hat{\tau}_y}{s_0 - \hat{\tau}_y}\right] - 1},$$

Integrated along constant strain rate path

$$\hat{\tau} = \hat{\tau}_s + \frac{1}{p}(s_0 - \hat{\tau}_y)\ln\left[1 - \left[1 - \exp\left(-p \frac{\hat{\tau}_s - \hat{\tau}_y}{s_0 - \hat{\tau}_y}\right)\right] \times \exp\left\{-\frac{p\theta\psi}{(s_0 - \hat{\tau}_y)\left[\exp\left(p \frac{\hat{\tau}_s - \hat{\tau}_y}{s_0 - \hat{\tau}_y}\right) - 1\right]}\right\}\right].$$

D.L. Preston, D.L. Tonks, D.C. Wallace, J. Appl. Phys. **93,** 211 (2003)

The PTW model fits to experimental data of low and high strain rates for copper

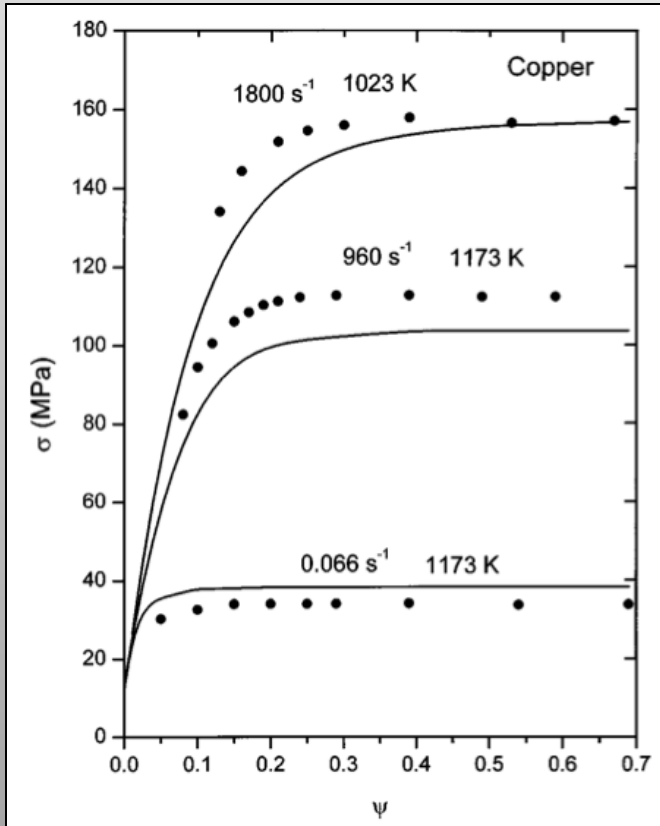

Comparison of the PTW model (solid lines) to the high-temperature stress-strain data of Samanta

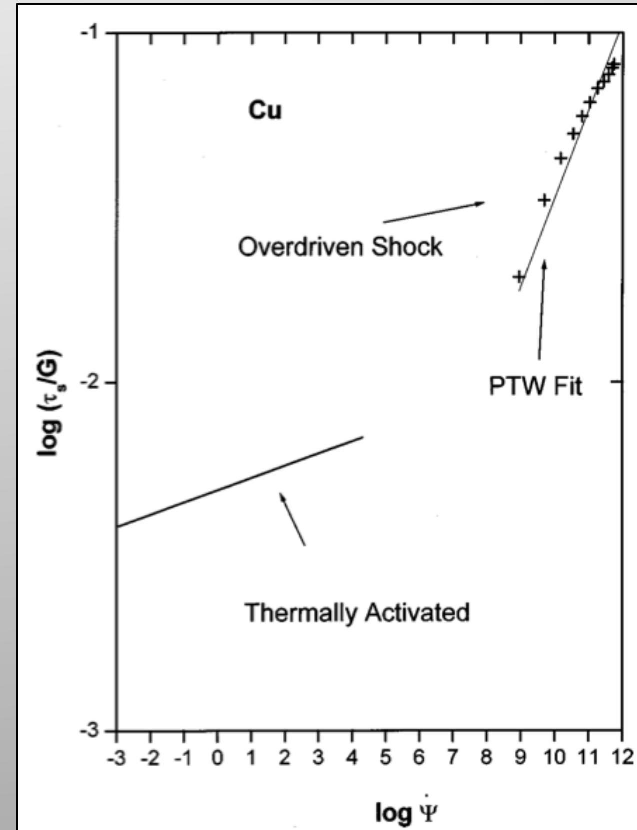

Copper saturation stress in the thermal-activation regime and over-driven shock results with the PTW model fit to those results

D.L. Preston, D.L. Tonks, D.C. Wallace, J. Appl. Phys. **93,** 211 (2003)

Laser compression on thin foils of vanadium induced blow-off, spall and fragmentation

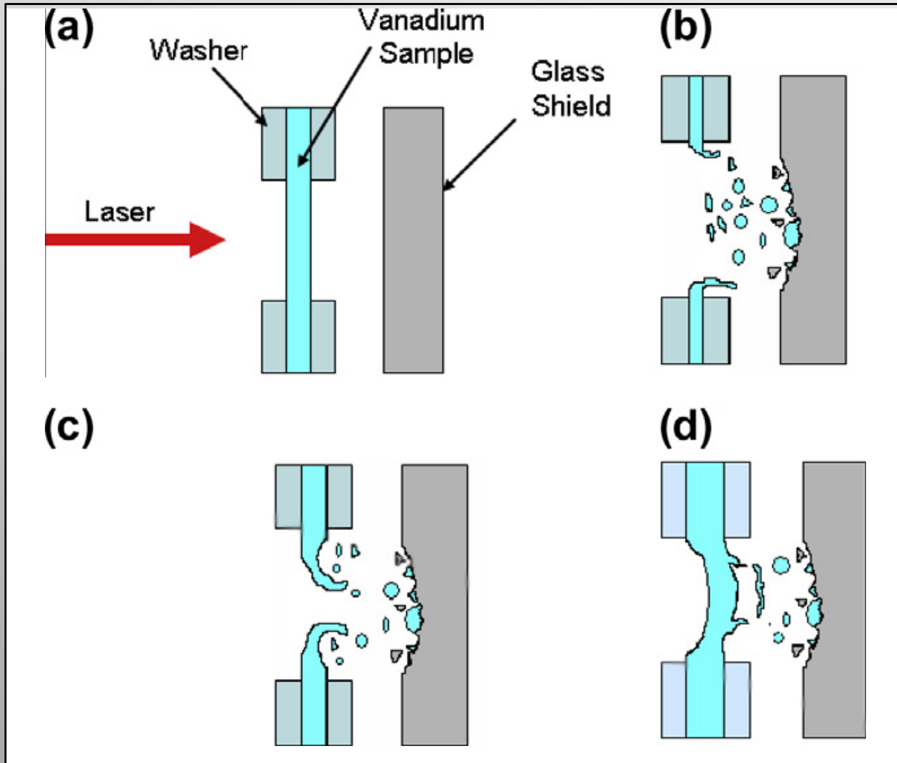

Schematic showing a) target setup; b) 75 um V foil blow-off completely; c) 127 um V foil showing both blow-off and spall; and d) 250 um V foil complete spall

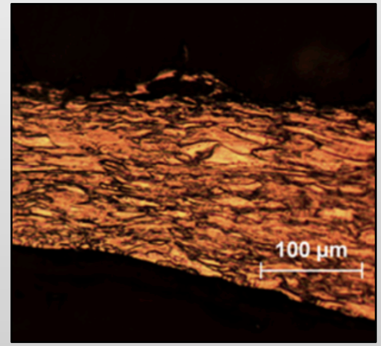

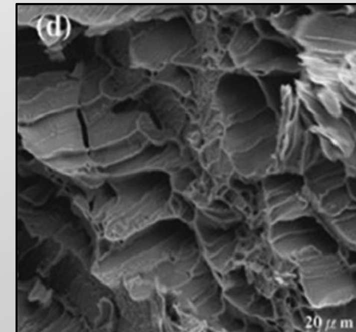

Flaking, separation along the grains, cracking and the formation of voids close to the surface are evident

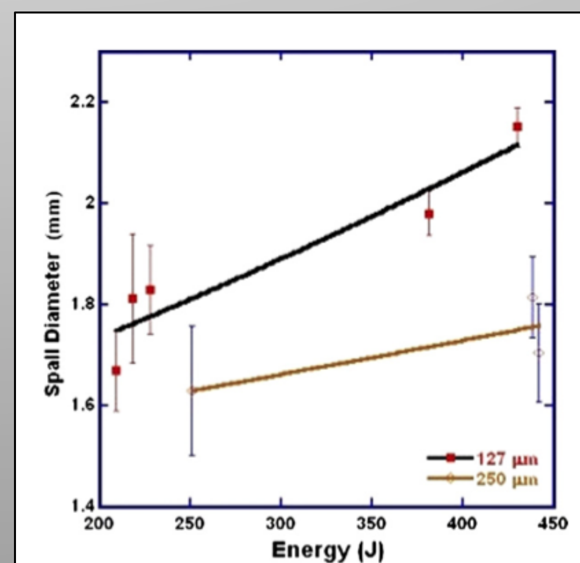

Spall diameter increases with increasing energy

H. Jarmakani, B. Maddox, C.T. Wei, D. Kalantar, M.A. Meyers, *Laser shocked-induced spalling and fragmentation in vanadium*, Acta Materialia, 2010

Material strength at very high pressures and strain rates have been demonstrated at Omega

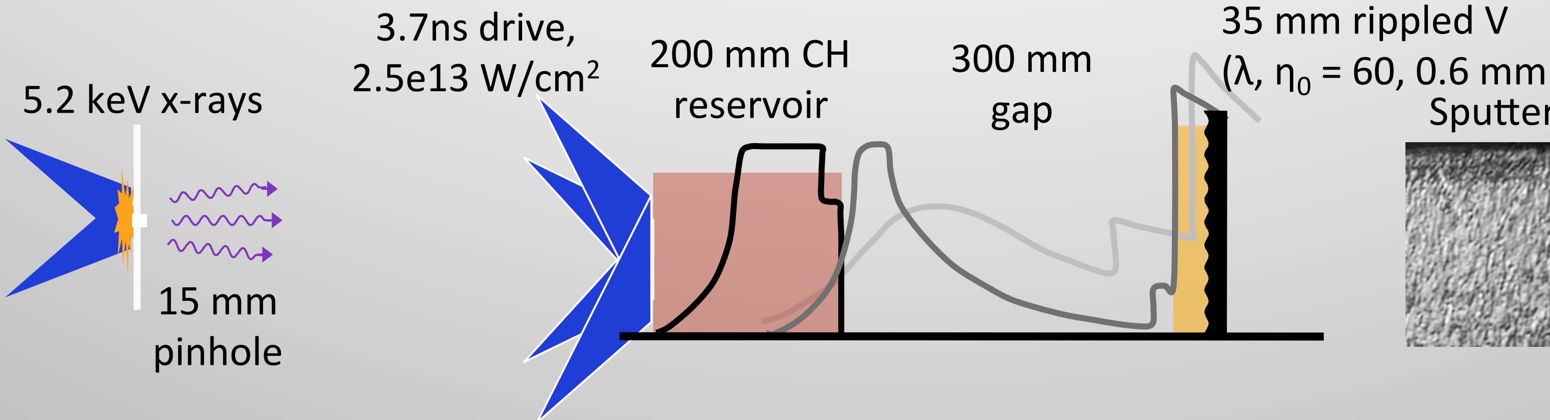

Sputtered V sample

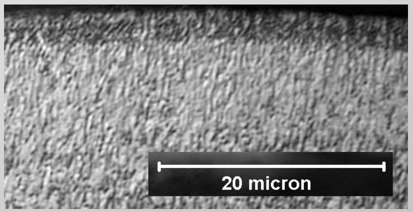

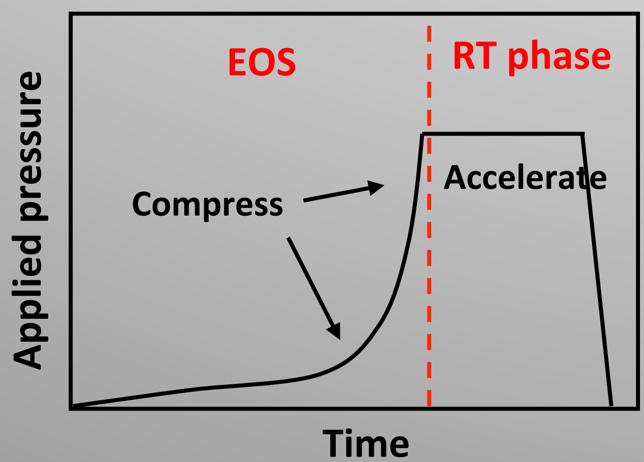

With material strength

No strength

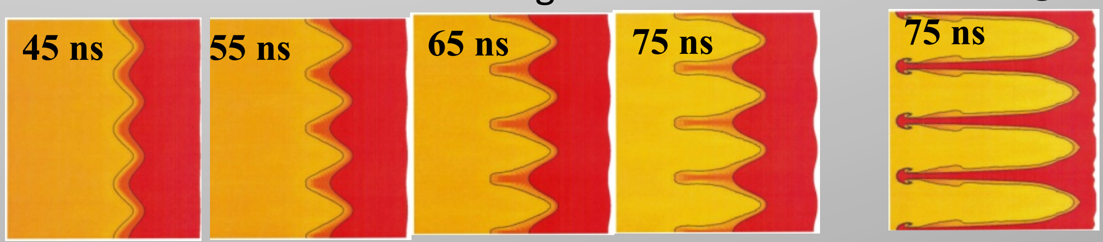

VISAR

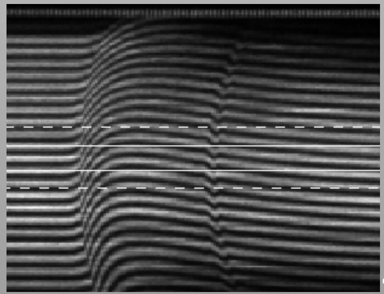

Face-on radiographs of ripple growth

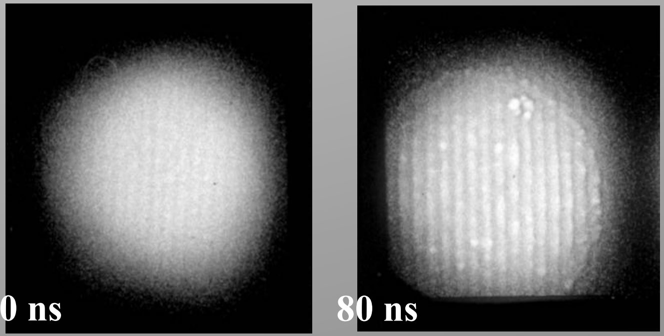

Strain rates order ~10% = 10^{-1}

Time scales around 10 ns

Characteristic strain rates = $10^{-1}/10^{-9}$ s = 10^{7} s^{-1}

[H.S. Park *et al.*, PRL 104, 135504 (2010)]

Experiments to check if Ta Raleigh Taylor experiments are sensitive to grain size effects at high pressures and strain rates

UCSD

- The Hall-Petch effect at ambient conditions is given by:

$$\sigma_{HP} = \sigma_0 + kD_{grain}^{-1/2}$$

- Following Zerilli-Armstrong, it is assumed the Hall-Petch effect is additive with strain and strain-rate hardening, and scales with G(P):

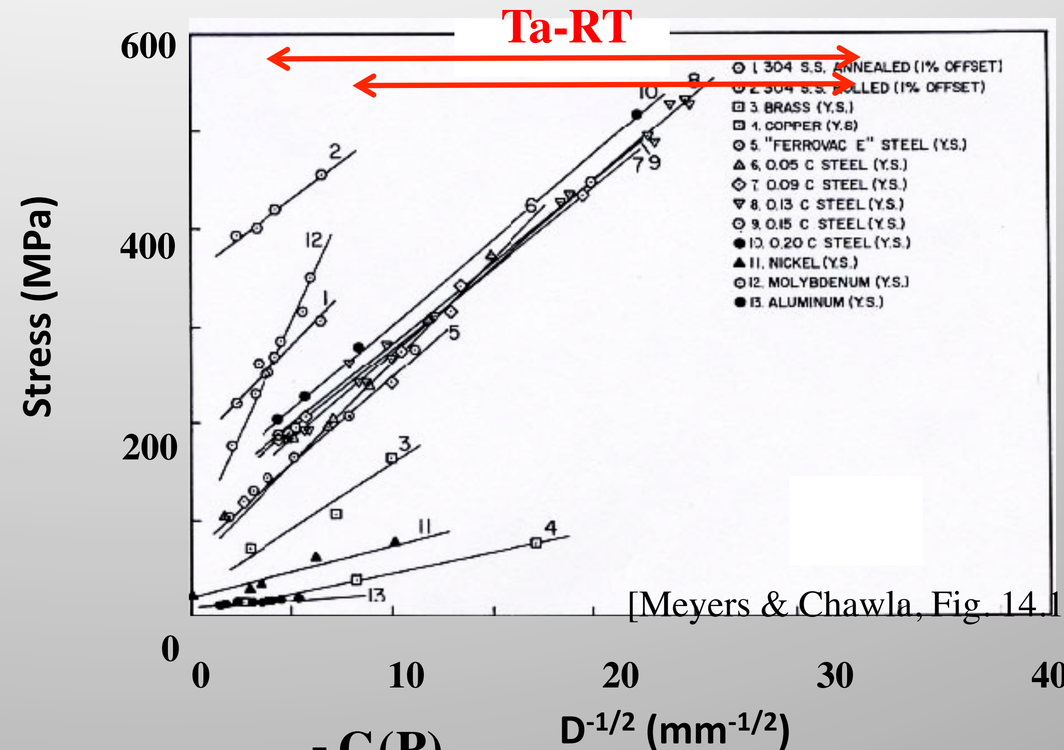

[Meyers & Chawla, Fig. 14.1]

$$\sigma_{ZA} = \left[\Delta\sigma'_G + c_1\exp(-c_3T + c_4T\dot{\varepsilon}) + c_5\varepsilon^n + kD_{grain}^{-1/2}\right]\frac{G(P)}{G_0}$$

- Assuming ambient conditions H-P parameters, the Hall-Petch effect is estimated to be only ~10% of the inferred peak strength for a 100x change in grain size for P_{max}~1 Mbar, de/dt ~10^7 s^{-1} TaRT experiment, which is below the experimental resolution.
- To check the grain size effect (to be sure), recent Omega shots were preformed to study the grain size effect in Ta-RT dynamics at ~1 Mbar, ~10^7 s^{-1} conditions

[B.A. Remington *et al.*, PRL 104, 135504 (2010)]

At the atomic scale MD can model voids, spall, dislocations and twins in structures with well defined potentials

Embedded Atom Method

$$E_i = F_\alpha\left(\sum_{i\neq j}\rho_\beta\left(r_{ij}\right)\right)+\frac{1}{2}\left(\sum_{i\neq j}\phi_{\alpha\beta}\left(r_{ij}\right)\right)$$

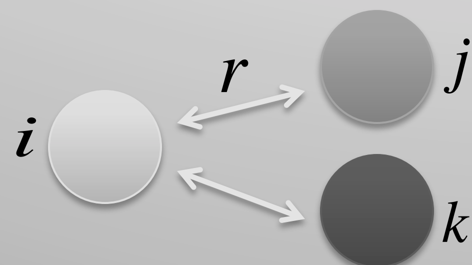

Periodic Boundary Condition: Unit cells are repeated for MD computations

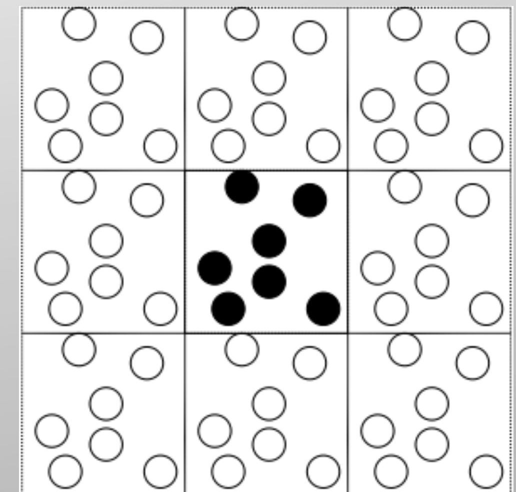

Cubic Sample

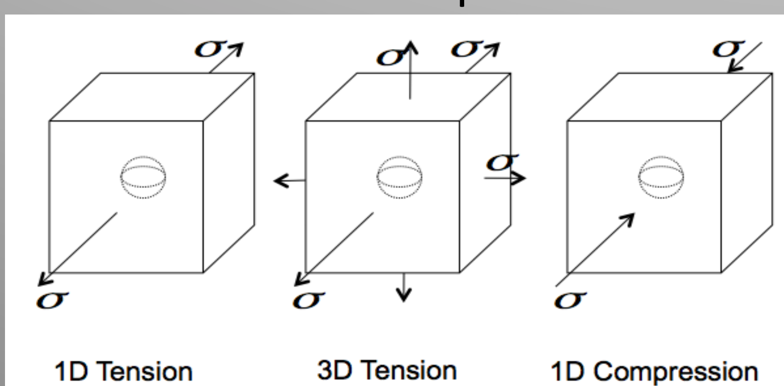

Void Growth in BCC Tantalum

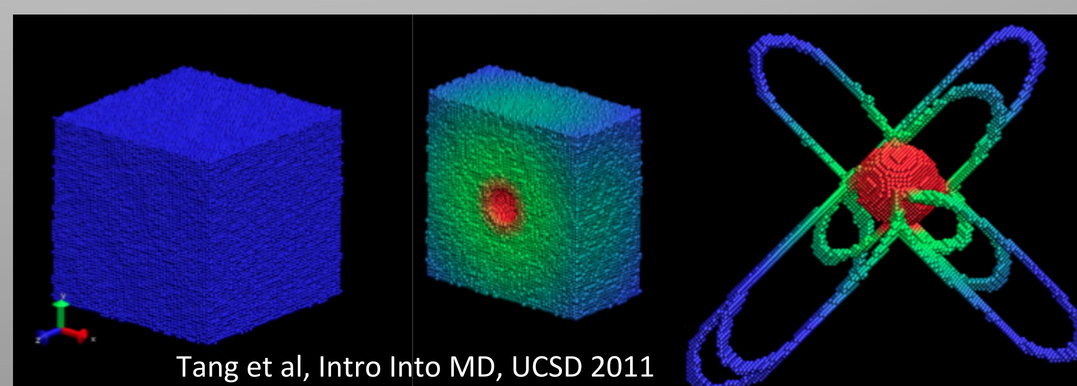

Hyades and Hydra are software tools that simulate the pressures throughout the sample during laser compression

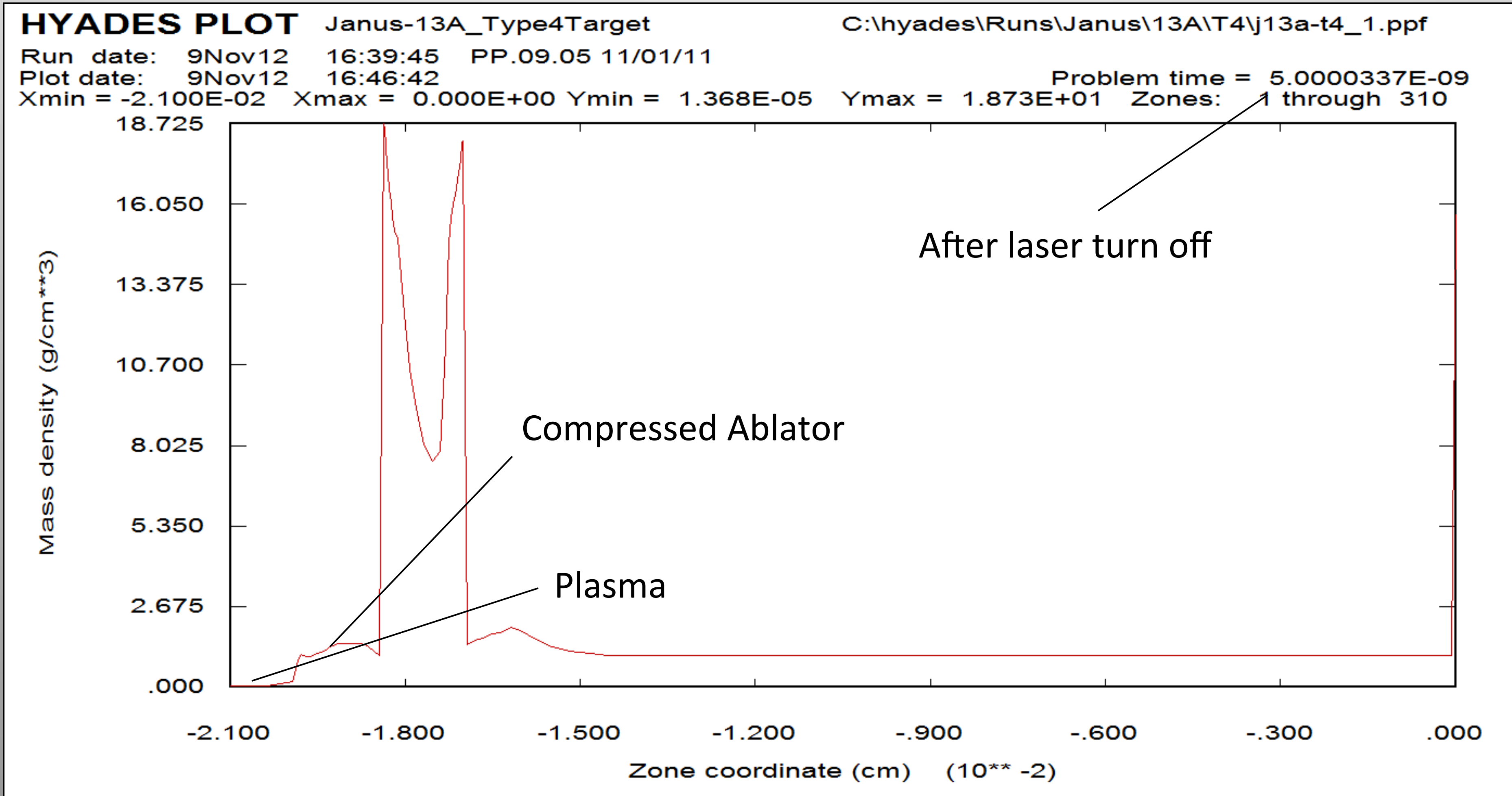

Wehrenberg, LLNL Janus 12B Hyades, 2012

VISAR is a velocity interferometer diagnostic to provide data on shock strength in experiments

Typical VISAR setup

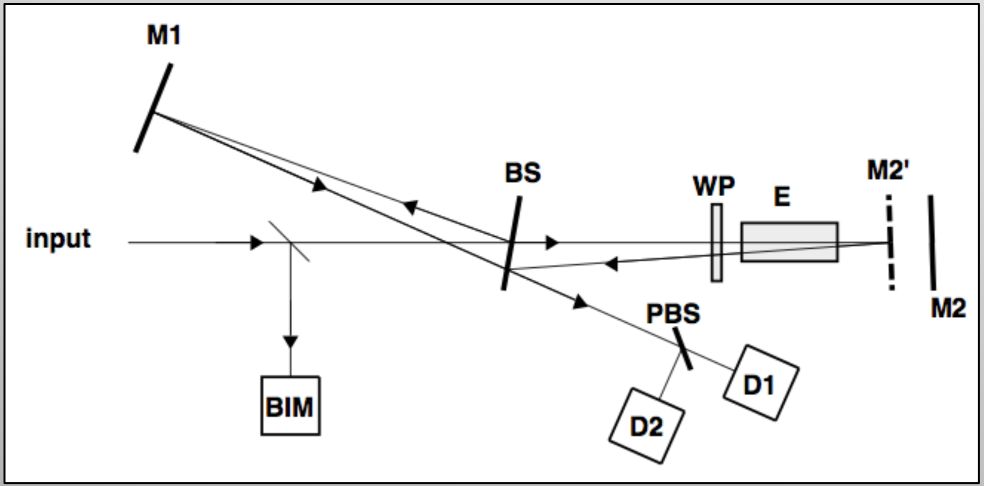

$$\frac{\lambda}{\lambda_0} = \frac{1 - \frac{v}{c_0}}{1 + \frac{v}{c_0}} \approx 1 - 2\frac{v}{c_0}$$

VISAR uses Hugoniot equations to determine:

- Spall strength
- Dynamic yield strengths
- Polymorphic phase transitions
- Shock induced melting
- Elastic constants at high pressures

λ = Reflected wavelength of light

λ_0 = Initial wavelength of light

v = Object velocity

c_0 = Speed of light

http://www.valynvisar.com/html/visar_applications.html

Experiments at extreme conditions are of particular interest for military and energy research

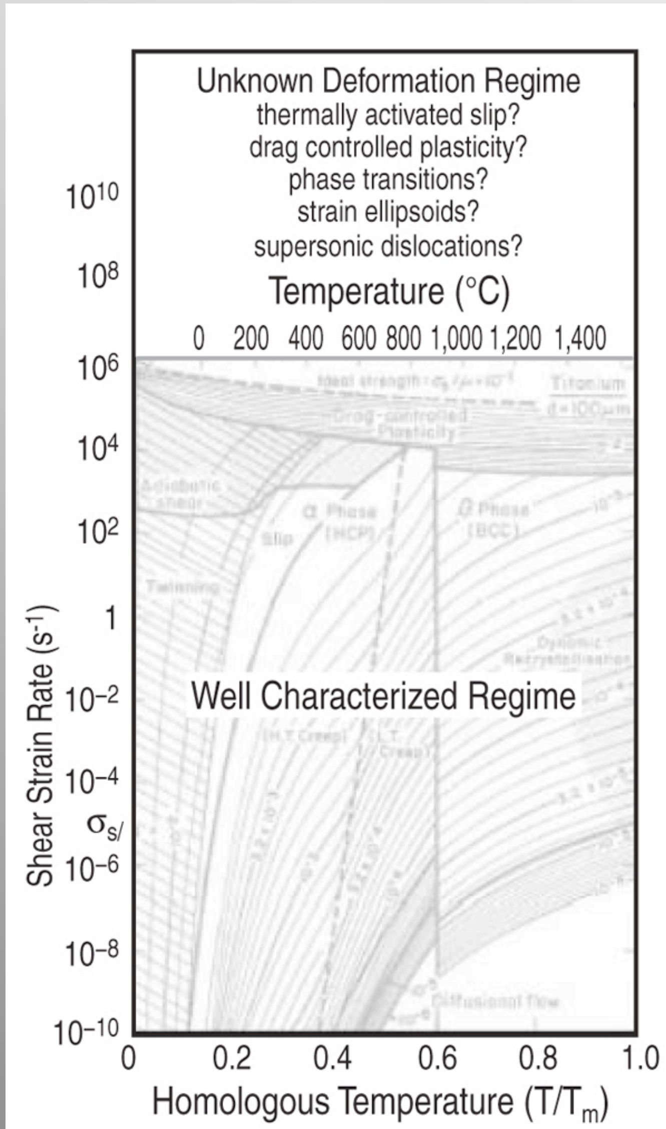

Inertial Confinement Fusion is the energy of the future

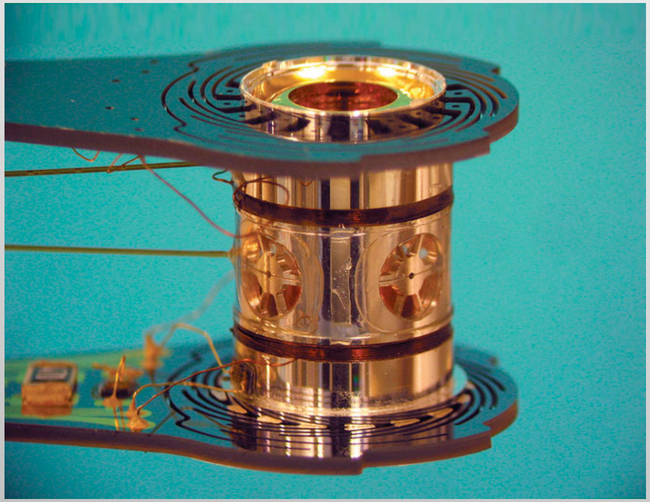

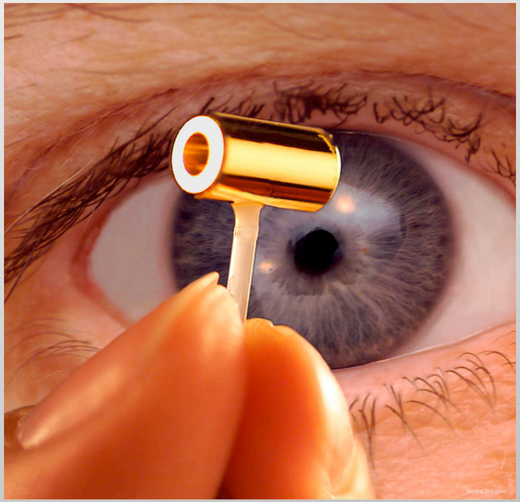

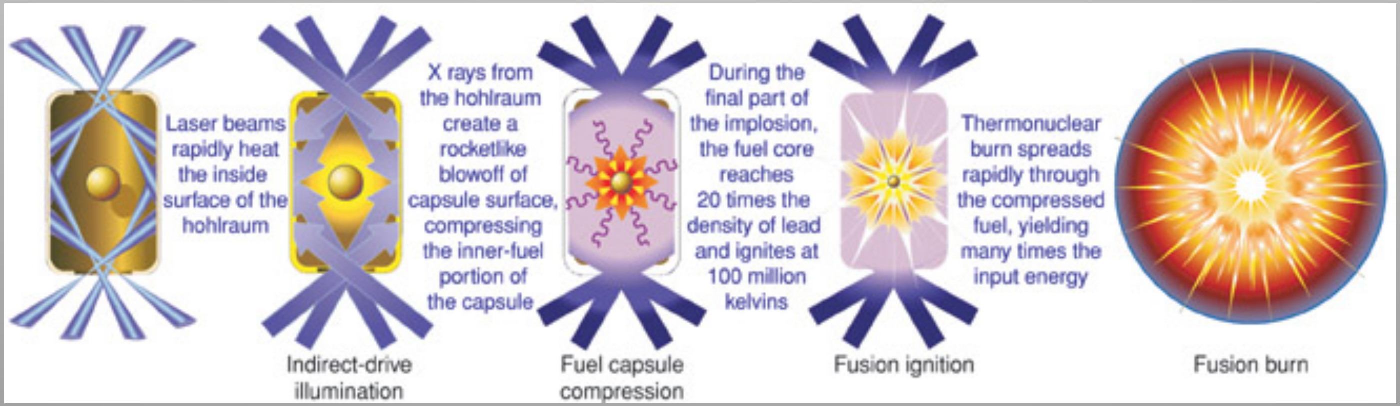

Summary

- Understanding the behavior of materials at high pressures, temperatures and strain rates is critical for many fields of science
- NIF is the largest laser in the entire world, scaling 3 football fields and has 192 laser beams with the capability of reaching 4 MJ in 5 ns
- Compression can be reached through direct, indirect, shock and ramp loading
- In 1963 Askaryon and Morez suggested that pulsed laser beams could produce recoil pressures from vaporization of metal surfaces
- White verified Askaryon's suggested effect on unconfined surfaces
- Anderholm showed that pressures of gigapascals could be obtained on confined surfaces (surfaces covered by a transparent overlay)
- Skeen and York demonstrated blow-off from laser shock
- 50 years of laser work has created a new field of materials science dedicated to materials behavior under laser compression
- There are many tools that help derive information from laser experiments such as hyades, hydra and molecular dynamic simulations as well as diagnostic setups such as VISAR
- Laser compression is essential for the future of the world's energy: ICF

Acknowledgments

Dr. Lubarda

Dr. Markenscoff

Dr. Meyers

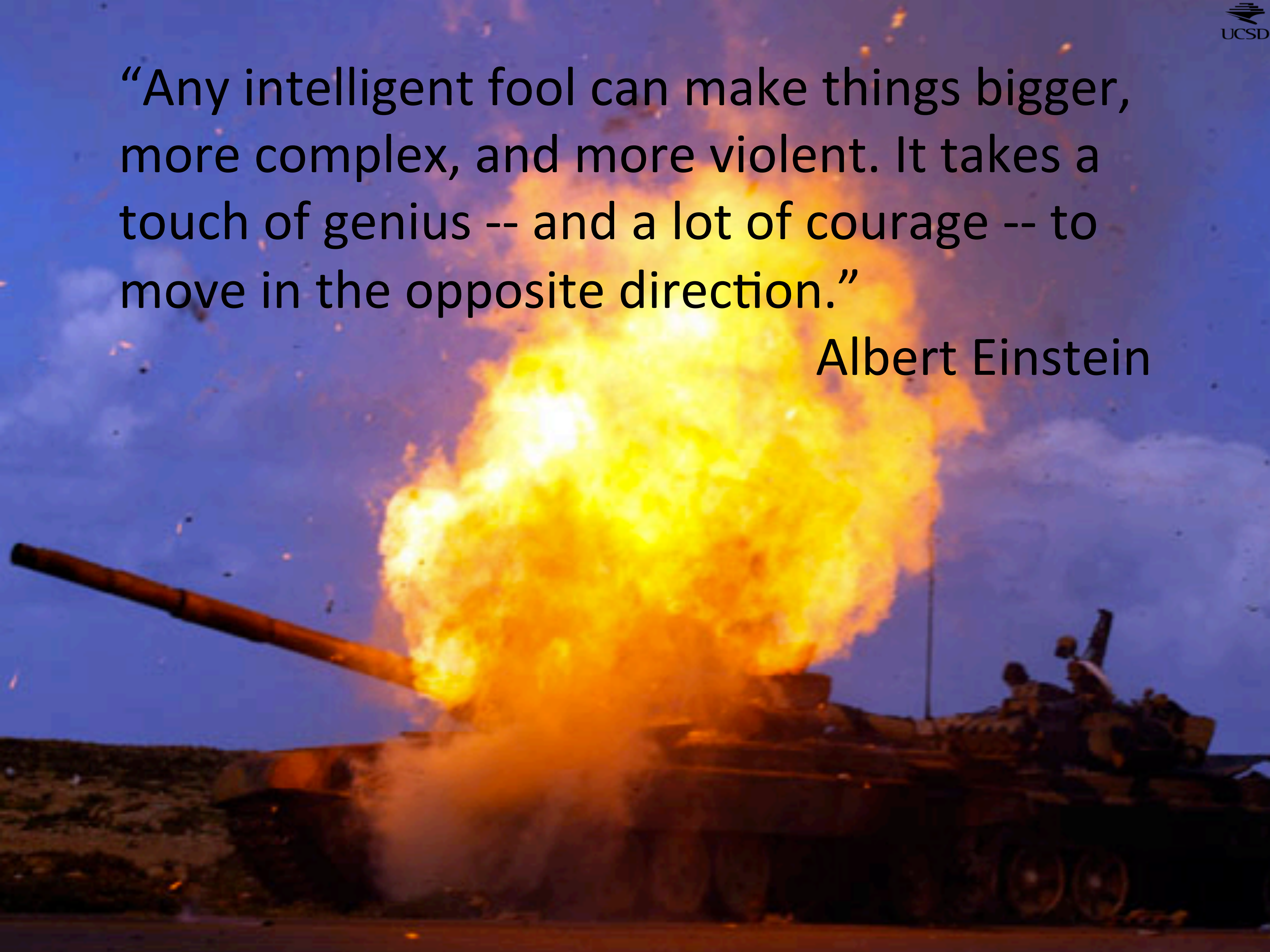
UCSD
"Any intelligent fool can make things bigger, more complex, and more violent. It takes a touch of genius -- and a lot of courage -- to move in the opposite direction."
Albert Einstein

The fusion reaction creates high temperature plasmas which are then transported to a power generator

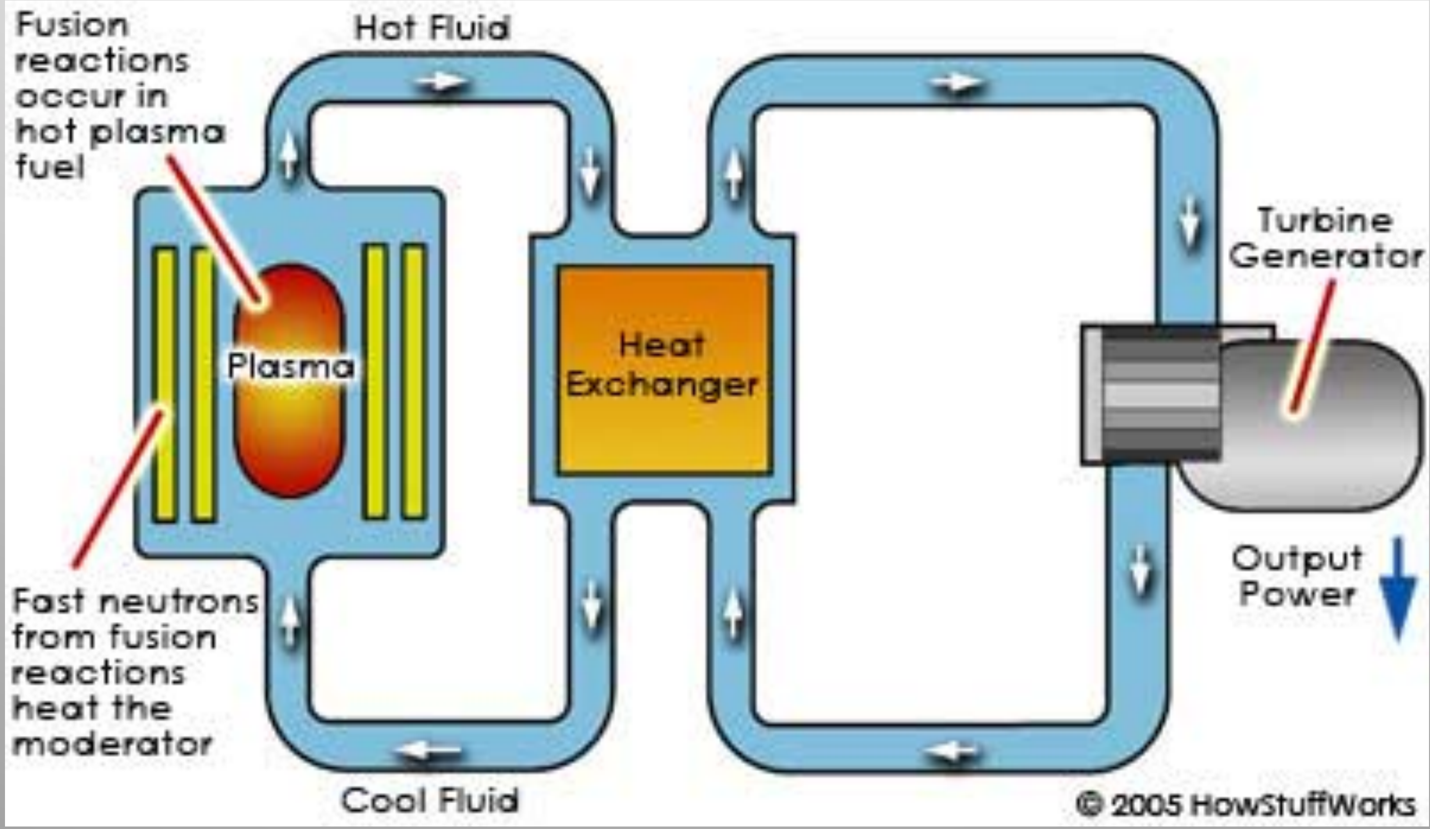

http://science.howstuffworks.com/fusion-reactor4.htm

In 1995 Vecchio studied the different material behavior of tantalum and tantalum alloys under laser compression

Optical micrographs of (a) annealed unalloyed-Ta, (b) annealed Ta-10W, (c) unalloyed-Ta shock loaded to 20 GPa, and (d) Ta-10W shock loaded to 20 GPa. Note the presence of deformation twins (arrows) introduced by the shock deformation. The wavy background structure observed in the Ta-10W samples is due to tungsten compositional fluctuations in the annealed plate material which result in differential etching behavior.

The propensity for long, straight screw dislocations, irrespective of the loading condition, supports the theory of strong Peierls stress control on defect generation and defect storage.

G.T. GRAY III and K. S. VECCHIO , Influence of Peak Pressure and Temperature on the Structure/Property Response of Shock-Loaded Ta and Ta-IOW, in Metallurgical and Materials Transactions A Volume 26, Number 10 (1995), 2555-2563

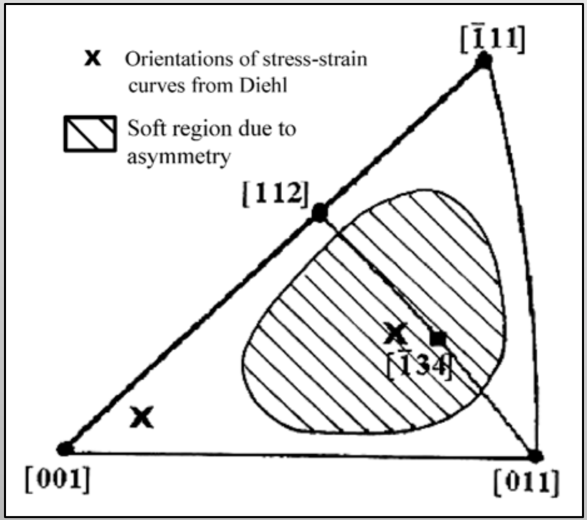
x Orientations of stress-strain curves from Diehl
Soft region due to asymmetry
[$\bar{1}$11]
[112]
[$\bar{1}$34]
[001]
[011]

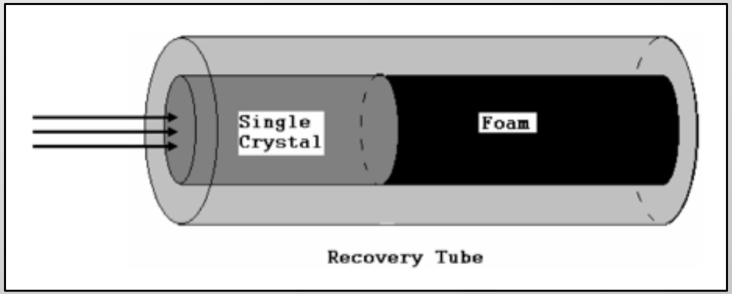
Single Crystal
Foam
Recovery Tube

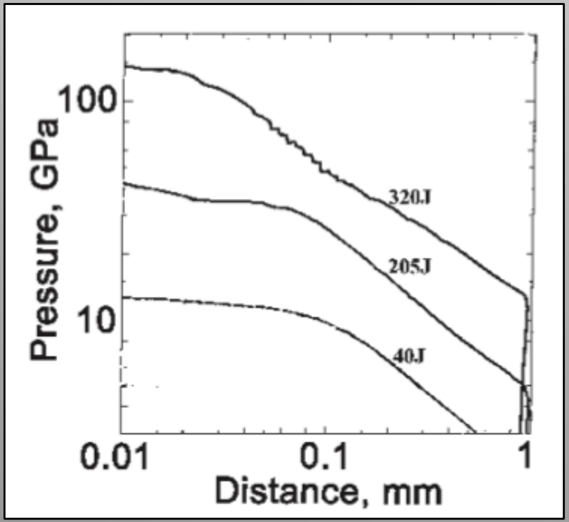
Pressure, GPa
100
10
320J
205J
40J
0.01
0.1
1
Distance, mm

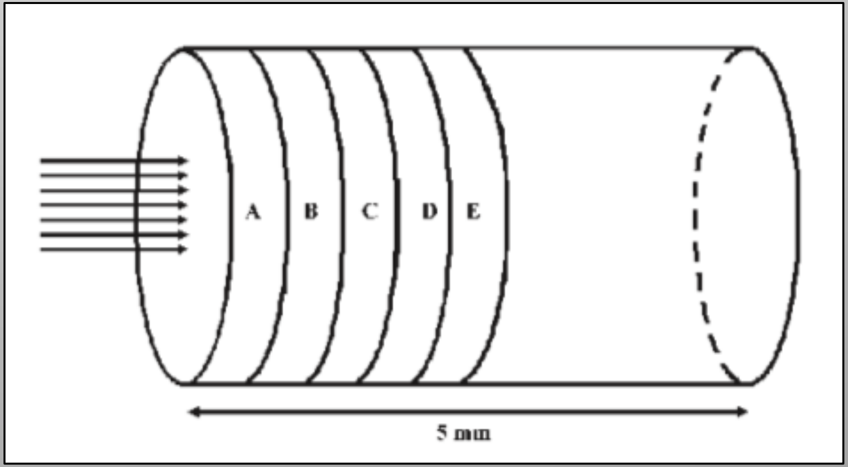
A
B
C
D
E
5 mm

Laser driven implosions can be either direct or indirect depending on the experiment

Direct Drive

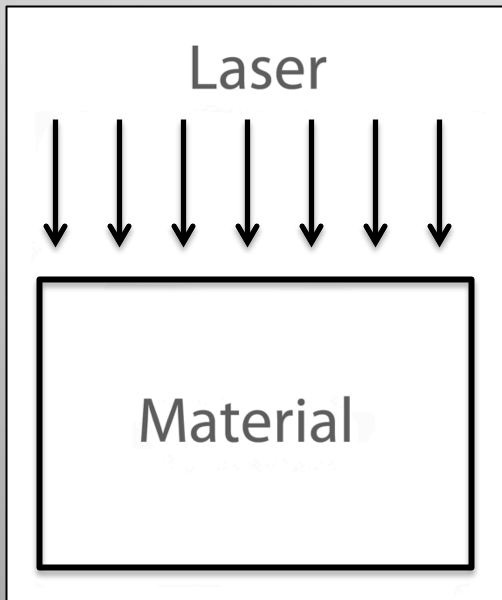

- Causes hot spots
- Trouble with smooth loading
- "Laser Imprinting"

Indirect Drive

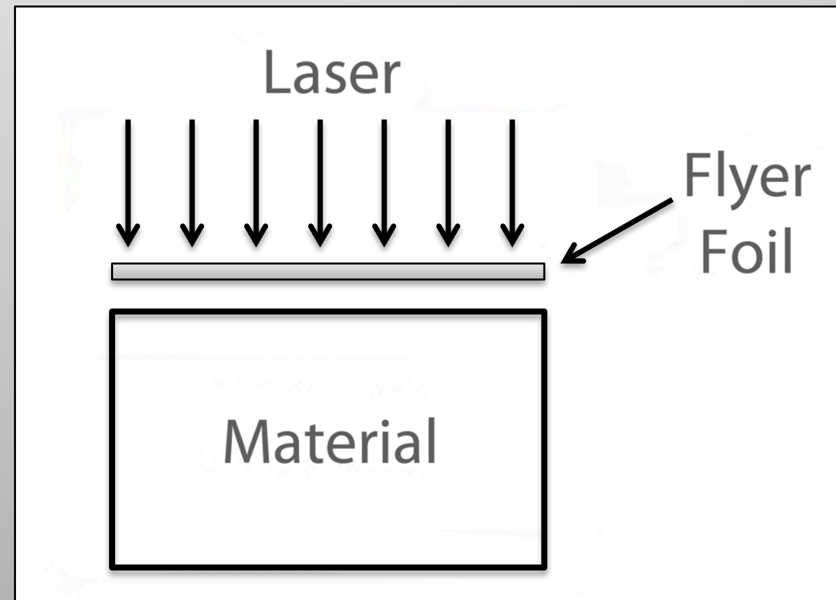

- Smooths out loading

By 2010 two novel methods became established to produce ramp compression from pulsed lasers

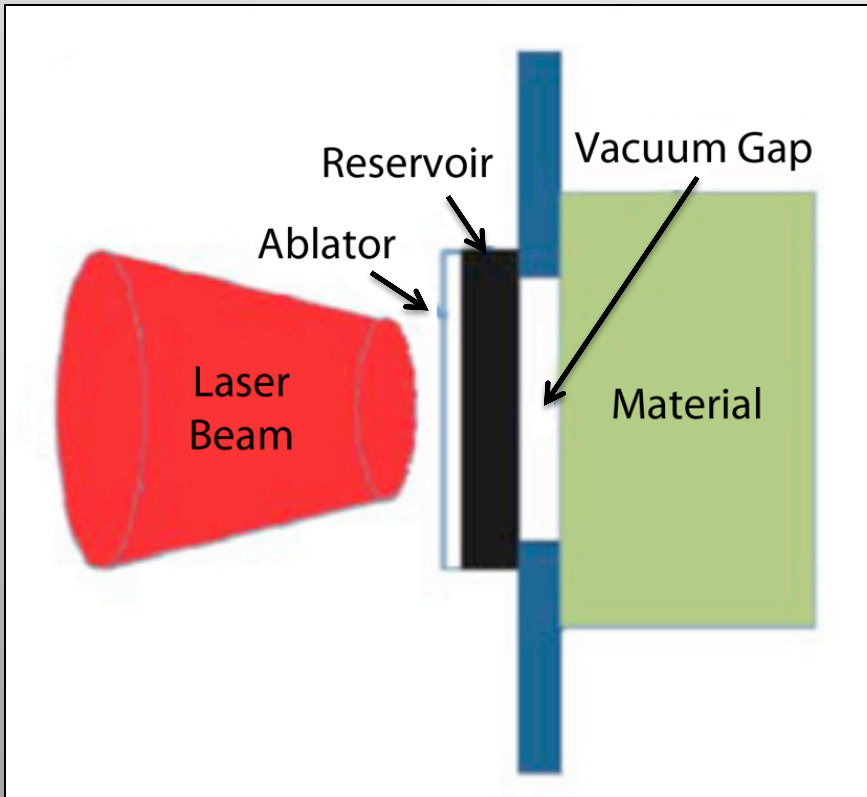

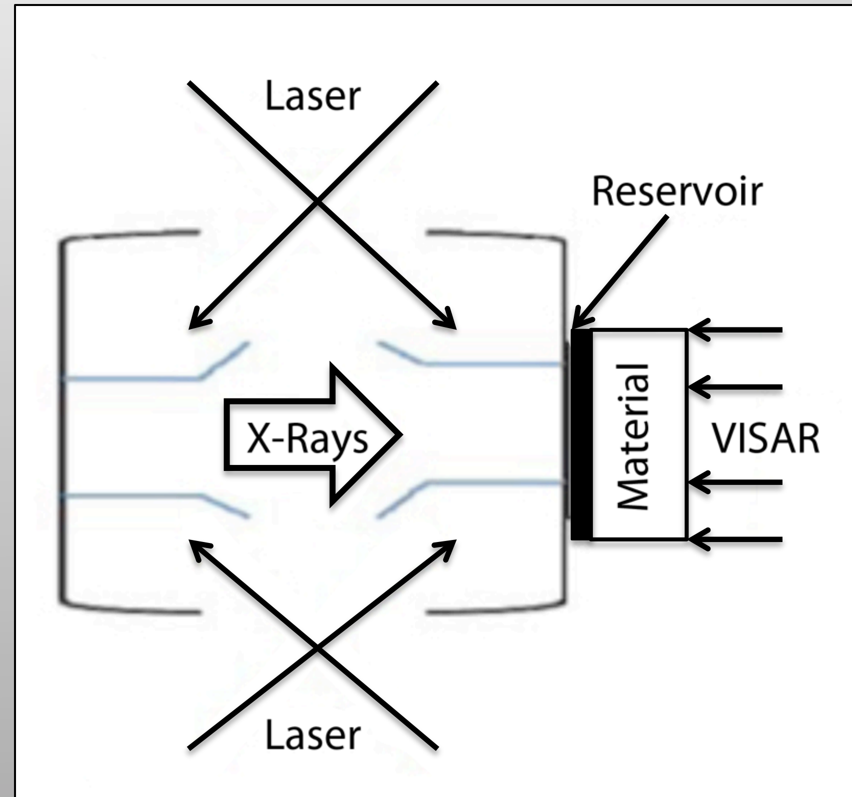

- Indirect loading created by ablator and vacuum gap

- Indirect loading created by soft x-rays